THE INFLUENCE OF DRILLED CAVITIES ON NATURAL CONVECTION AND SATURATED POOL BOILING HEAT TRANSFER FROM A HORIZONTAL SURFACE

George Richard Yount

NAVAL POSTGRADUATE SCHOOL
Monterey, California

THESIS

THE INFLUENCE OF DRILLED CAVITIES ON
NATURAL CONVECTION AND SATURATED
POOL BOILING HEAT TRANSFER FROM
A HORIZONTAL SURFACE

by

George Richard Yount

December 1976

Thesis Advisor: M. Kelleher

SECURITY CLASSIFICATION OF THIS PAGE (When Date Entered)

REPORT DOCUMENTATION PAGE

READ INSTRUCTIONS BEFORE COMPLETING FORM

1. REPORT NUMBER

2. GOVT ACCESSION NO.

3. RECIPIENT'S CATALOG NUMBER

4. TITLE (and Subtitle)
The Influence of Drilled Cavities on Natural Convection and Saturated Pool Boiling Heat Transfer from a Horizontal Surface

5. TYPE OF REPORT & PERIOD COVERED
Master's Thesis; December 1976

6. PERFORMING ORG. REPORT NUMBER

7. AUTHOR(s)
George Richard Yount

8. CONTRACT OR GRANT NUMBER(s)

9. PERFORMING ORGANIZATION NAME AND ADDRESS
Naval Postgraduate School
Monterey, California 93940

10. PROGRAM ELEMENT, PROJECT, TASK AREA & WORK UNIT NUMBERS

11. CONTROLLING OFFICE NAME AND ADDRESS
Naval Postgraduate School
Monterey, California 93940

12. REPORT DATE
December 1976

13. NUMBER OF PAGES
92

14. MONITORING AGENCY NAME & ADDRESS(if different from Controlling Office)
Naval Postgraduate School
Monterey, California 93940

15. SECURITY CLASS. (of this report)
Unclassified

15a. DECLASSIFICATION/DOWNGRADING SCHEDULE

16. DISTRIBUTION STATEMENT (of this Report)
Approved for public release; distribution unlimited.

17. DISTRIBUTION STATEMENT (of the abstract entered in Block 20, if different from Report)

18. SUPPLEMENTARY NOTES

19. KEY WORDS (Continue on reverse side if necessary and identify by block number)

20. ABSTRACT (Continue on reverse side if necessary and identify by block number)

The objective of this research project was to study the effect of small artificial cavities on both natural convection and the incipience of saturated pool boiling from a horizontal test surface. All tests were run with distilled Freon 113. Data for the heat flux as a function of the superheat and the convection heat transfer coefficient as a function of the heat flux were carefully obtained and plotted.

DD FORM 1 JAN 73 1473 EDITION OF 1 NOV 68 IS OBSOLETE
S/N 0102-014-6601 |
(Page 1)

SECURITY CLASSIFICATION OF THIS PAGE (When Date Entered)

Experimental results are presented for the heat transfer from horizontal circular disks, with and without artificial cavities.

Increases in both natural convection and boiling heat transfer were observed with the addition of artificial cavities. The magnitude of heat transfer augmentation was found to be strongly dependent upon the artificial cavity density.

THE INFLUENCE OF DRILLED CAVITIES ON NATURAL CONVECTION AND SATURATED POOL BOILING HEAT TRANSFER FROM A HORIZONTAL SURFACE

by

George Richard Yount
Lieutenant, United States Navy
B.S., Industrial Education, 1968

Submitted in partial fulfillment of the requirements for the degree of

MASTER OF SCIENCE IN MECHANICAL ENGINEERING

from the

NAVAL POSTGRADUATE SCHOOL
December 1976

ABSTRACT

The objective of this research project was to study the effect of small artificial cavities on both natural convection and the incipience of saturated pool boiling from a horizontal test surface. All tests were run with distilled Freon 113. Data for the heat flux as a function of the superheat and the convection heat transfer coefficient as a function of the heat flux were carefully obtained and plotted. Experimental results are presented for the heat transfer from horizontal circular disks, with and without artificial cavities.

Increases in both natural convection and boiling heat transfer were observed with the addition of artificial cavities. The magnitude of heat transfer augmentation was found to be strongly dependent upon the artificial cavity density.

TABLE OF CONTENTS

LIST OF TABLES

LIST OF FIGURES

NOMENCLATURE

SYMBOL	DESCRIPTION	UNITS
A	Any surface area of interest	Ft^2
D	Inside diameter of glass cylinder	Ft
d	Outside diameter of test surface central core	Ft
h	Convection heat transfer coefficient	BTU/ hr ft^2 ^oF
h_1	Convection heat transfer coefficient over one inch central core	BTU/ hr ft^2 ^oF
h_2	Convection heat transfer coefficient over the circumferential fin	BTU/ hr ft^2 ^oF
$I_\nu(x)$	Modified Bessel function	
Kss	Thermal conductivity of type 304 Austenetic stainless steel	BTU/ hr ft ^oF
$K_\nu(x)$	Modified Bessel function	
m	Quantity equal to $[h/Kss\ w]^{\frac{1}{2}}$	1/Ft
Q	Heat transfer rate	BTU/hr
q	Heat flux	BTU/hr ft^2
Qin	Heat transfer rate into the test surface	BTU/hr
Qloss	Heat transfer rate lost through the circumferential fin	BTU/hr
Qout	Heat transfer rate out of the one inch central core of the test surface	BTU/hr
r	Radius at any point of interest on the test surface	Ft
r_B	Radius of the test surface at the base of the circumferential fin	Ft
TC1-6	Thermocouples 1-6 in the test surface central core	
TC5-6	Thermocouples 5 and 6. Two closest to the boiling surface	

Tsat	Fluid saturation temperature	^{o}F
Tss	Temperature of stainless steel Test surface as measured by $\frac{TC6 + TC5}{2}$	^{o}F
TS1	Test surface 1	
TS2	Test surface 2	
Tw	Boiling surface temperature	^{o}F
w	Circumferential fin thickness	Ft
x	Bessel function argument (mr_B)	
ΔT	Temperature variation between TC5 and TC6	^{o}F
$\Delta Tsat$	Superheat ($\Delta Tsat = Tw - Tsat$)	^{o}F
$\Delta Tsat1$	Superheat over the central core	^{o}F
$\Delta Tsat2$	Superheat over the circumferential fin	^{o}F
Δx	Axial distance along the test surface core	Ft
θ	Temperature difference ($T - Tsat$)	^{o}F
θ_o	Temperature difference ($T_o - Tsat$)	^{o}F

ACKNOWLEDGEMENT

In any work of this nature the advances to be made are realized only with the combined efforts of many individuals. The author of this paper wishes to thank the following individuals for their contributions: Professor M. D. Kelleher, his thesis advisor, for his guidance and assistance throughout this work; Professor P. J. Marto for his sage technical advice and Mr. George F. Bixler for his outstanding skill as a craftsman and as a quality machinist.

Special thanks and grateful appreciation is due to my wife, Kathleen, for her perseverance in a most trying time and to my children, Kimberly and Joseph, for allowing me the liberty to selfishly use a portion of their precious youth.

I. INTRODUCTION

A. BACKGROUND

With the discovery of the characteristic boiling curve in 1934, boiling heat transfer research has become an area of intensive investigation.

Throughout the past 42 years investigators have been actively engaged in efforts to identify all the physical and geometric parameters involved with boiling heat transfer. Consistent with this effort has been the equally difficult task of finding meaningful and descriptive relationships among these parameters that would enable better correlation of all experimental data. The boiling curve, as shown in figure 1, is generally described by the following four major regions: natural convection, nucleate boiling, transition boiling and stable film boiling. For most practical engineering purposes only the natural convection and nucleate boiling regions are of significant interest. It is in these regions, and in particular the upper portion of the nucleate boiling region, for which industrial equipment utilizing boiling heat transfer is designed. The inherent instability and potentially dangerous burnout conditions that prevail at the end of the nucleate boiling region make this area as well as the transition and film boiling regions undesirable for practical application.

In most boiling processes, phase transition (change from liquid to vapor) does not occur precisely at the saturation

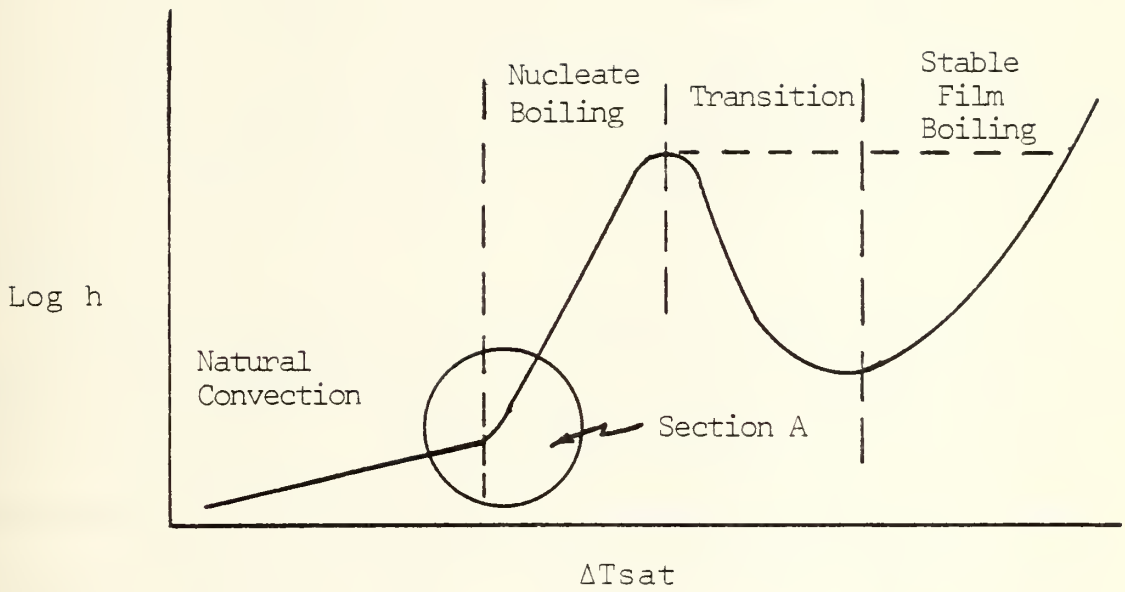

Figure 1. Characteristic Boiling Curve

point of the liquid. This phenomenon generally manifests itself in a certain amount of increased temperature of the heated surface above the fluid saturation temperature in order to initiate boiling. This increased temperature is referred to as superheat (temperature difference, ΔT_{sat}, between the wall temperature, T_w, and the fluid saturation temperature, T_{sat}).

The superheat condition is governed primarily by the pressure of the liquid and the number of places on the surface (called nucleation sites) where gas bubbles can form. This entire process is a metastable state in phase transition; and it is for this reason that once the nucleation of vapor occurs and nucleate boiling is established, there are dramatic changes in the heat transfer properties of the system.

Generally speaking the inception of boiling displays itself as the characteristic "knee" of the boiling curve, section A of figure 1. This portion of the curve is altered somewhat by the rather high superheat condition required to activate nucleation sites. Once a site has been activated, a small amount of vapor remains in the site due to surface tension. The presence of this vapor allows the boiling process to continue and causes a marked decrease in the superheat required to sustain the boiling process. This change in the superheat requirements is generally displayed as a hysteresis loop as shown in figure 2. In this figure line ABEC represents the ideal transition from natural convection to nucleate boiling heat transfer. ABDEC represents the

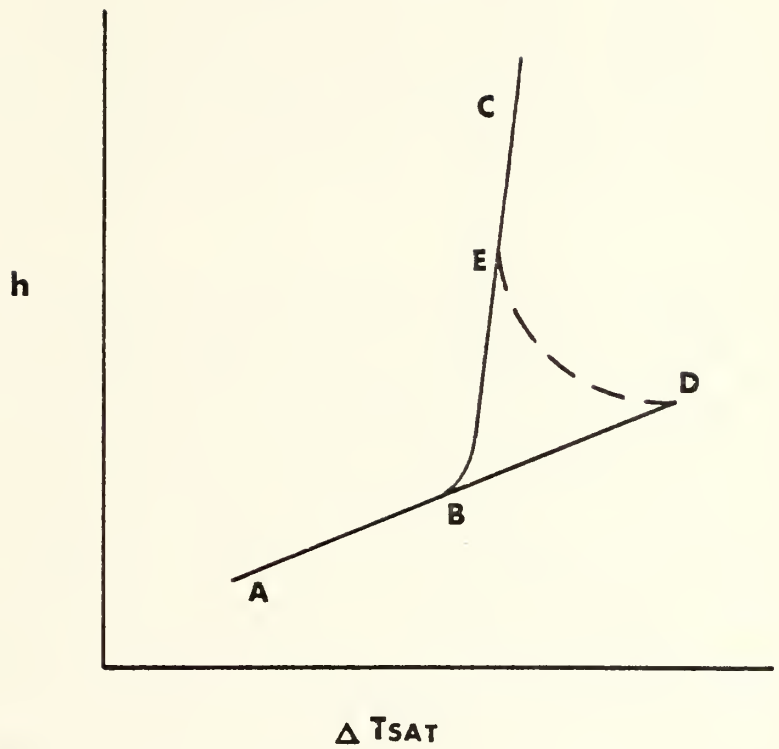

Figure 2. Metastable Superheat Condition

hysteresis loop formed as a result of the superheat required to cause nucleation. Line ABEC also represents the situation in which nucleate boiling is well established and the temperature of the surface is decreased until all nucleation sites deactivate. The characteristic path followed in this case is CEBA.

In situations of low superheat, natural convection predominates as the heat transfer mode and is associated with low heat fluxes, $q \alpha \Delta T_{sat}^{4/3}$ [1]. In this segment of the boiling curve the driving force for the fluid motion is the buoyant force created by density differences of the fluid [2].

Nucleate boiling is characterized by a sharp rise in the heat transfer coefficient with a moderate rise in the superheat. This situation is sometimes referred to as the high heat flux region represented by $q \alpha \Delta T_{sat}^{3.3}$ [1]. During this phase, bubbles are created by expansion of entrapped gas or vapor at small cavities in the surface. These bubbles grow to some critical size which is a function of the temperature, pressure and the surface tension at the liquid vapor interface [3].

In saturated, or bulk, boiling, the fluid motion is driven by the separation of the vapor bubbles from the surface and their subsequent rise through the fluid due to buoyant forces. Once the bubbles detach and rise, they agitate the fluid in such a way as to cause an updraft of hot liquid to follow in their wake. As the flow situation

develops, the steady upflow of liquid above the nucleation site leads to a steady downflow of liquid towards the heat transfer surface. This flow system is responsible for the fluid motion being radial toward the nucleation site where it rises again [1,3]. This flow pattern is illustrated in figure 3.

In the region of high heat flux, principally after the establishment of nucleate boiling, a small increase in superheat brings a large increase in the heat transfer coefficient. This displays itself phenomenologically in the form of increased frequency of bubble generation. As the frequency of bubble departure increases, a point is reached when there is a coalescence of the bubbles, i.e. bubble generation and separation occur so rapidly that the bubbles collide forming a single, continuous vapor column. This will, of course, occur in both the vertical and lateral direction. From the previous discussion on bubble generation, it is readily apparent that at some point in time the generation of bubbles from nucleation sites becomes so intense as to develop a continuous vapor film across the heat transfer surface. Due to the extremely poor conductivity of gases, the presence of a vapor film or "blanket" over the heat transfer surface causes the heat transfer from the surface to decrease substantially. Once the heat transfer surface has been more or less insulated by the vapor blanket, the continued build-up of heat within the system generally results in temperatures that could exceed the melting temperature of the surface causing catastrophic failure of the heat transfer surface by burnout.

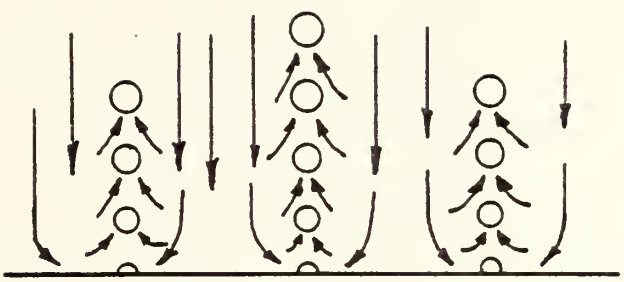

Figure 3. Fluid Flow Pattern in Nucleate Boiling

B. PREVIOUS RESEARCH

In the regions of natural convection and nucleate boiling, it has been observed that many factors affect ths shape of the boiling curve. A partial listing of these factors include such parameters as number and distribution of nucleation sites, surface material, surface conditions, past boiling history of the surface, aging effects of the surface, fluid depth, fluid temperature, fluid surface tension and system geometry.

In an attempt to discover the pertinent relationships between the various boiling parameters, Corty and Foust [4] investigated the boiling of organic liquids in a transparent rectangular plastic test vessel. They observed hysteresis effects and a shifting of the boiling curve to give a steeper slope for the heat transfer coefficient versus superheat than had been previously noted.

In both pool and flow boiling experiments conducted with fluorocarbons [5], hysteresis effects similar to those reported by Corty and Foust [4] were observed. These effects were attributed to the superheat condition and cavity deactivation (a nucleation site that has ceased to produce bubbles).

Experiments by Marto, Moulson and Maynard [6] involving the boiling of liquid nitrogen from a mirror finished heat transfer surface with artificial cavities showed that an increase in the number of drilled cavities improves the heat transfer from the surface. They also observed a further increase in the heat transfer coefficient as the cavity size

was increased. Shoukri and Judd [7] in their work on nucleation site activation concluded that smaller cavities were better able to trap gas vapor and be activated by their local neighbors once boiling is established.

Experiments conducted by Heled, Ricklis and Orell [1] investigating pool boiling from large arrays of artificial nucleation sites produced results in both the natural convection and nucleate boiling regions. In the natural convection region, they, like Marto, Moulson and Maynard [6], found a marked improvement in the heat transfer from such prepared surfaces. In the nucleate boiling region they observed that the boiling heat transfer rate at any given superheat could be increased by varying the site density of the artificial nucleation sites. This increasing of the heat transfer rate is, of course, not a boundless phenomenon. As discussed in the previous section, bubble generation eventually becomes so vigorous as to form a film of vapor over the heat transfer surface markedly reducing its effectiveness.

In all experimental boiling heat transfer research, there is still great difficulty in getting a true and absolute correlation between experimental results. Perhaps the most significant problem in this regard is the extremely difficult task of quantifying the surface finish on the test section and its effect on the heat transfer characteristics of the surface. This is a problem well recognized by researchers and one that influenced the results of this project.

The objective of this research project was to investigate the influence of small artificial cavities on both natural

convection and the incipience of saturated pool boiling of Freon 113 from a horizontal test surface.

II. EXPERIMENTAL APPARATUS

The experimental apparatus employed in this study is shown in figure 4. The major components of the system are a data acquisition and power supply unit, a thermocouple switching box and the experimental unit.

The data acquisition unit consists of a Hewlett Packard Dymec model 2401B integrating digital voltmeter, a Hewlett Packard model 562A digital recorder and a Harrison Laboratories, Inc., model 809A 0-36 volt, 0-10 amp regulated power supply. This unit functioned to supply and monitor power to the test surface heater block and to display and record thermocouple output in millivolts.

An external view of the assembled experimental unit is shown in figure 5, and a labeled cross-sectional view of this same unit is shown in figure 6. As depicted in figure 6, the major components of the experimental unit are the cylindrical fluid tank, reflux condenser, fluid bulk heater, test surface and test surface heater block.

Figure 7 is a top view of the cylindrical fluid tank showing the relative position of both the fluid bulk heater and the circular test surface. The fluid bulk heater was constructed of Nichrome wire wrapped around ceramic stand-off insulators. The operation of the bulk heater was controlled by a Variac.

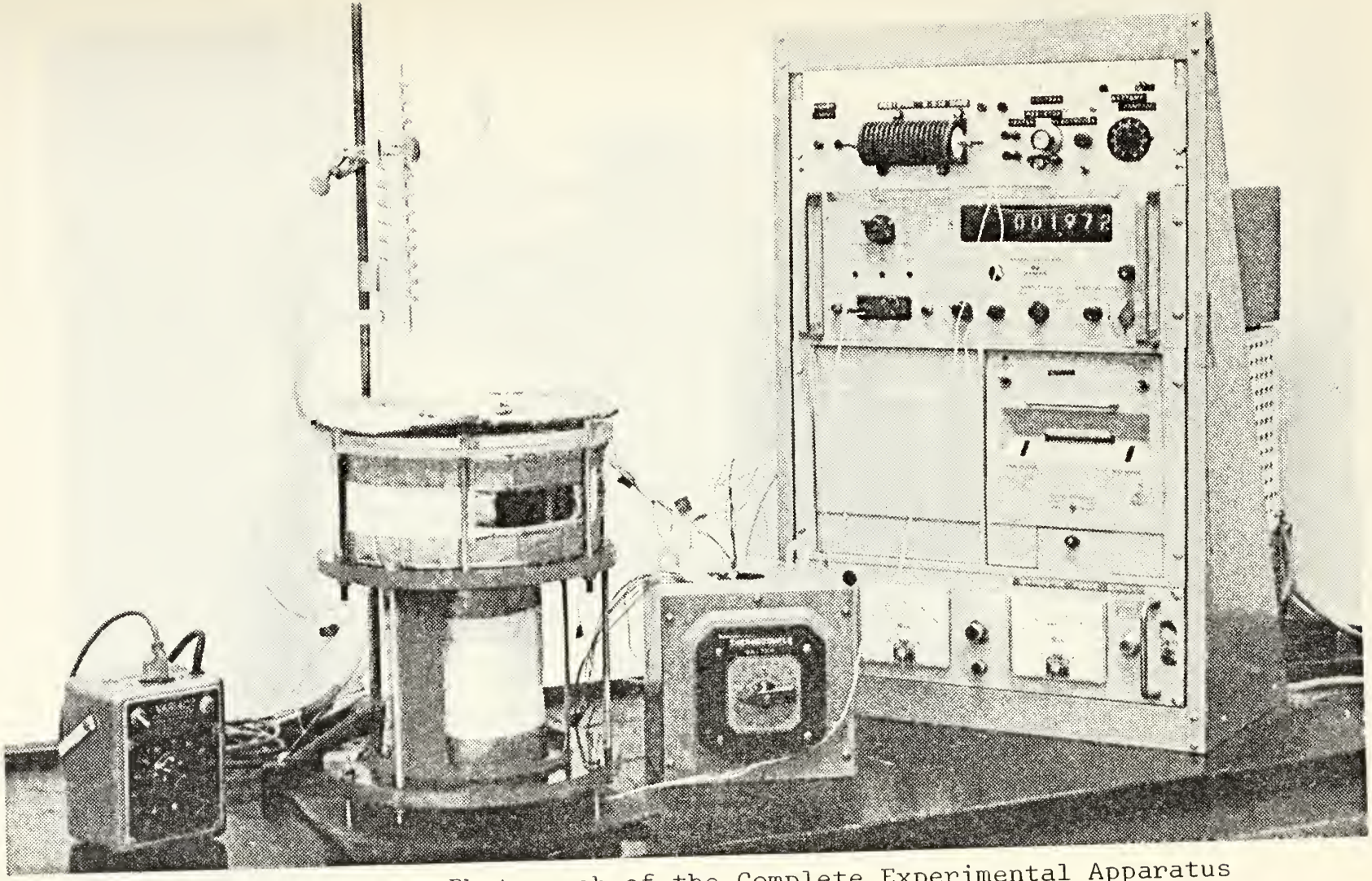

Figure 4. Photograph of the Complete Experimental Apparatus

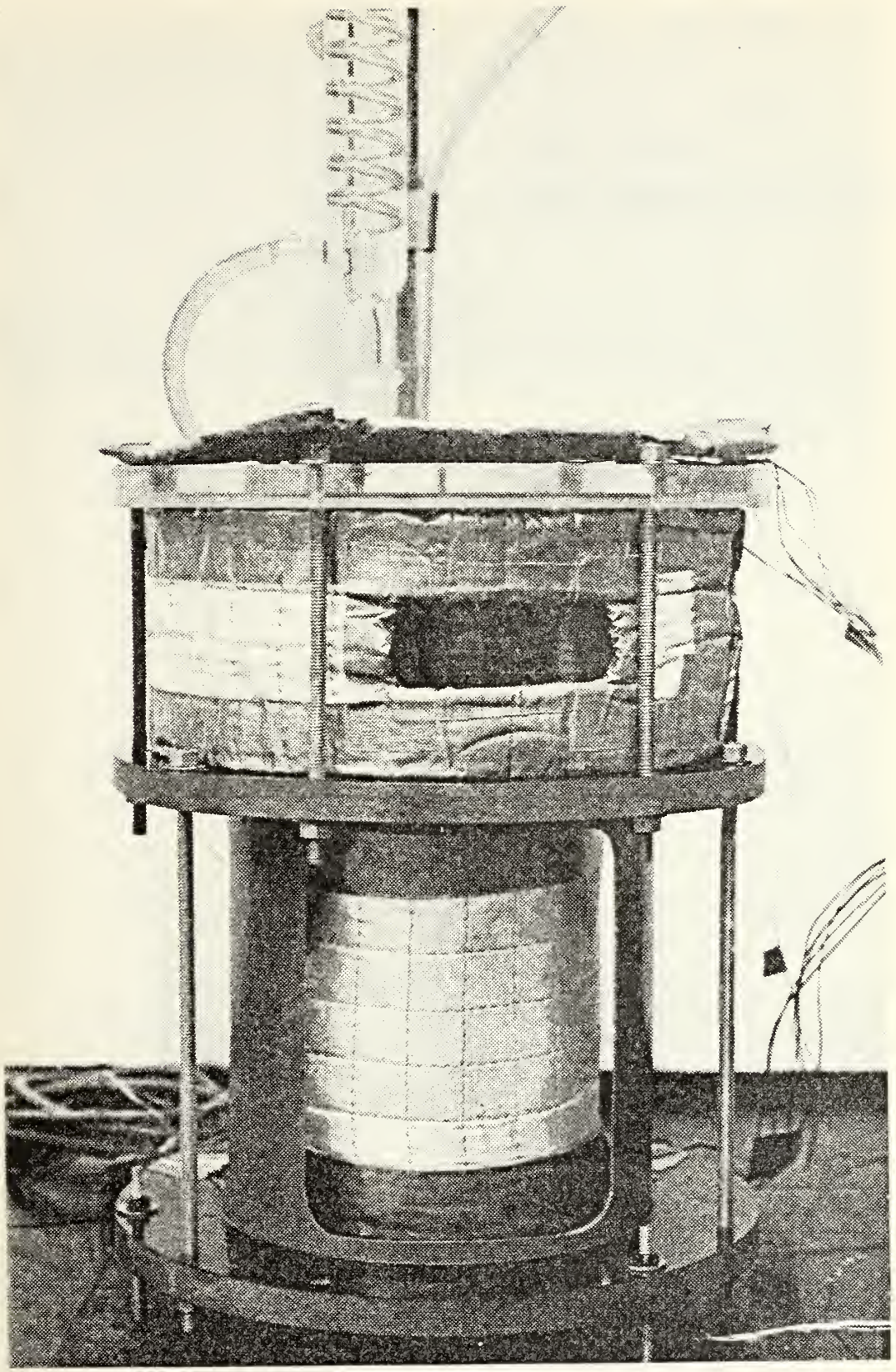

Figure 5. Photograph of the Assembled Experimental Unit

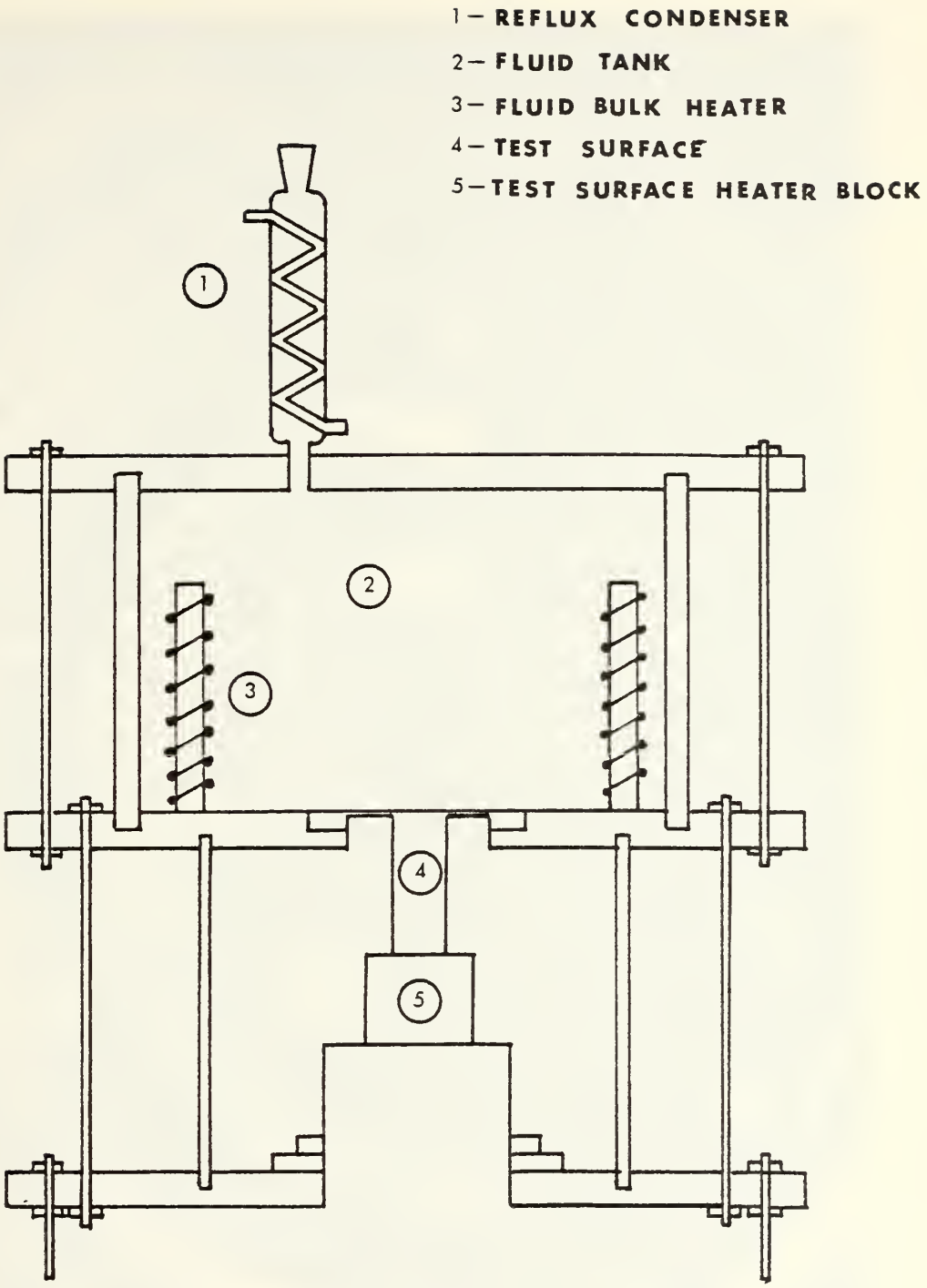

Figure 6. Cross-Sectional View of the Experimental Unit

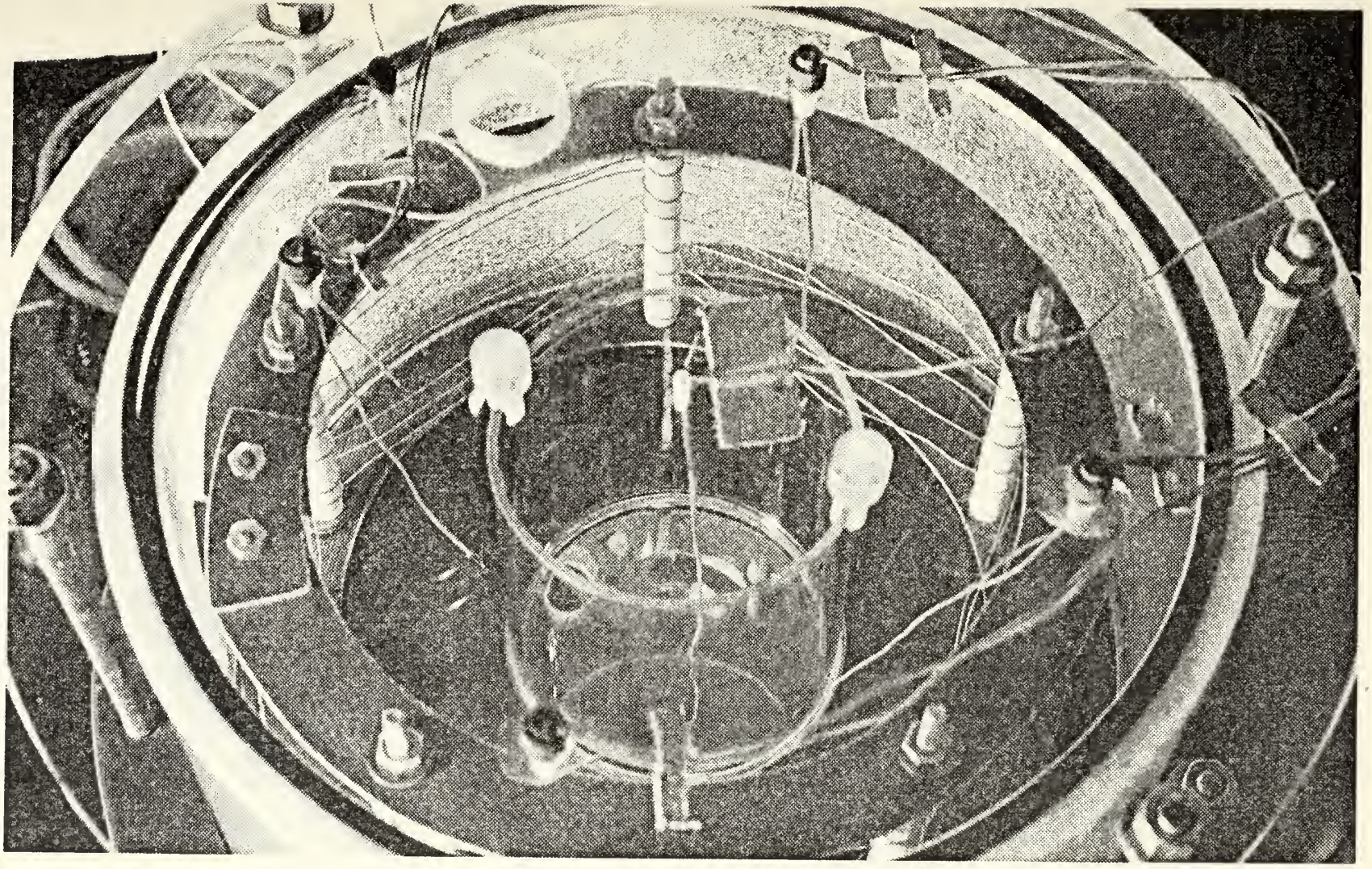

Figure 7. Photograph from Top of Fluid Tank Showing Position of Fluid Bulk Heater and the Test Surface

The test surface itself is the most significant member of the experimental unit. Figure 8 is a generalized cross-sectional view of the surface. The test surface was constructed of type 304 austenitic stainless steel with the actual boiling surface being both hand lapped and machine polished to a mirror finish. Aside from providing a surface from which to boil, the test surface acts as a heat flux metering device allowing a calculation of the boiling surface temperature of the test section. In an attempt to minimize conduction and radiation losses, the entire lower portion of the experimental unit, consisting of the underside of the test surface and the test surface heater block, was heavily insulated by first wrapping all components with several layers of asbestos cloth and then applying five layers of 0.250 inches (0.635 cm) MIN-K insulation.

A. TEST SURFACE

The test surface used in this experiment is an amalgamation of surfaces used by previous investigators [8,9,10,11]. The dominating influence in the design of the test surface was the design used by Chapman [8] in his pool and flow boiling experiments. The major refinement to Chapman's design was the development of a machining procedure whereby a homogeneous test surface could be fabricated.

Figure 9 illustrates the geometry of the test surface and the placement of the thermocouple wells. As can be seen from the figure, the test surface is basically a 1 inch (2.54 cm) central core with an extremely thin circumferential fin, on

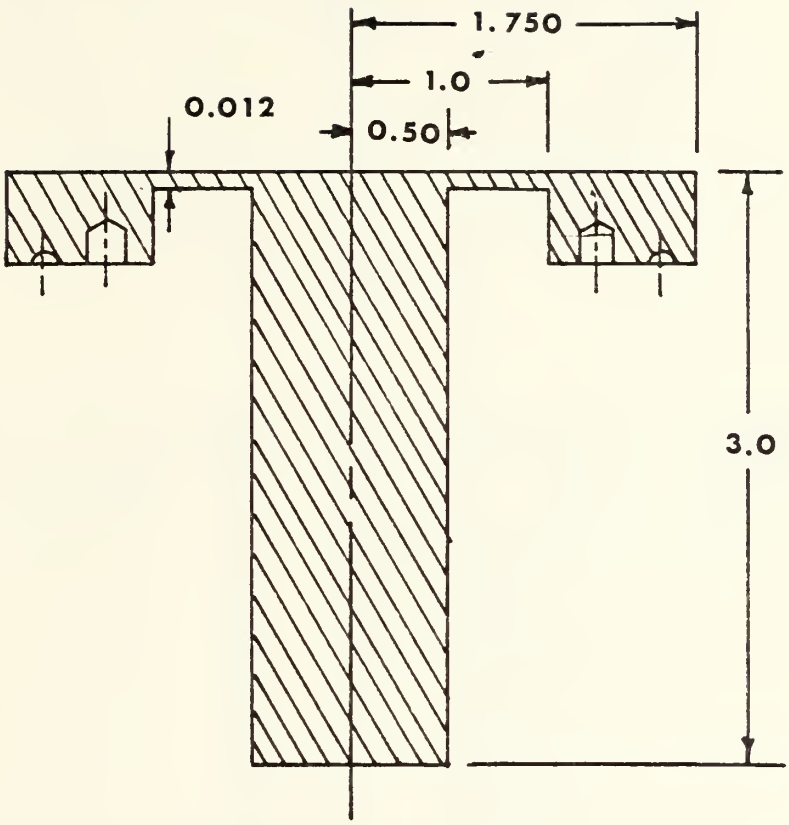

Figure 8. Test Surface without Thermocouples

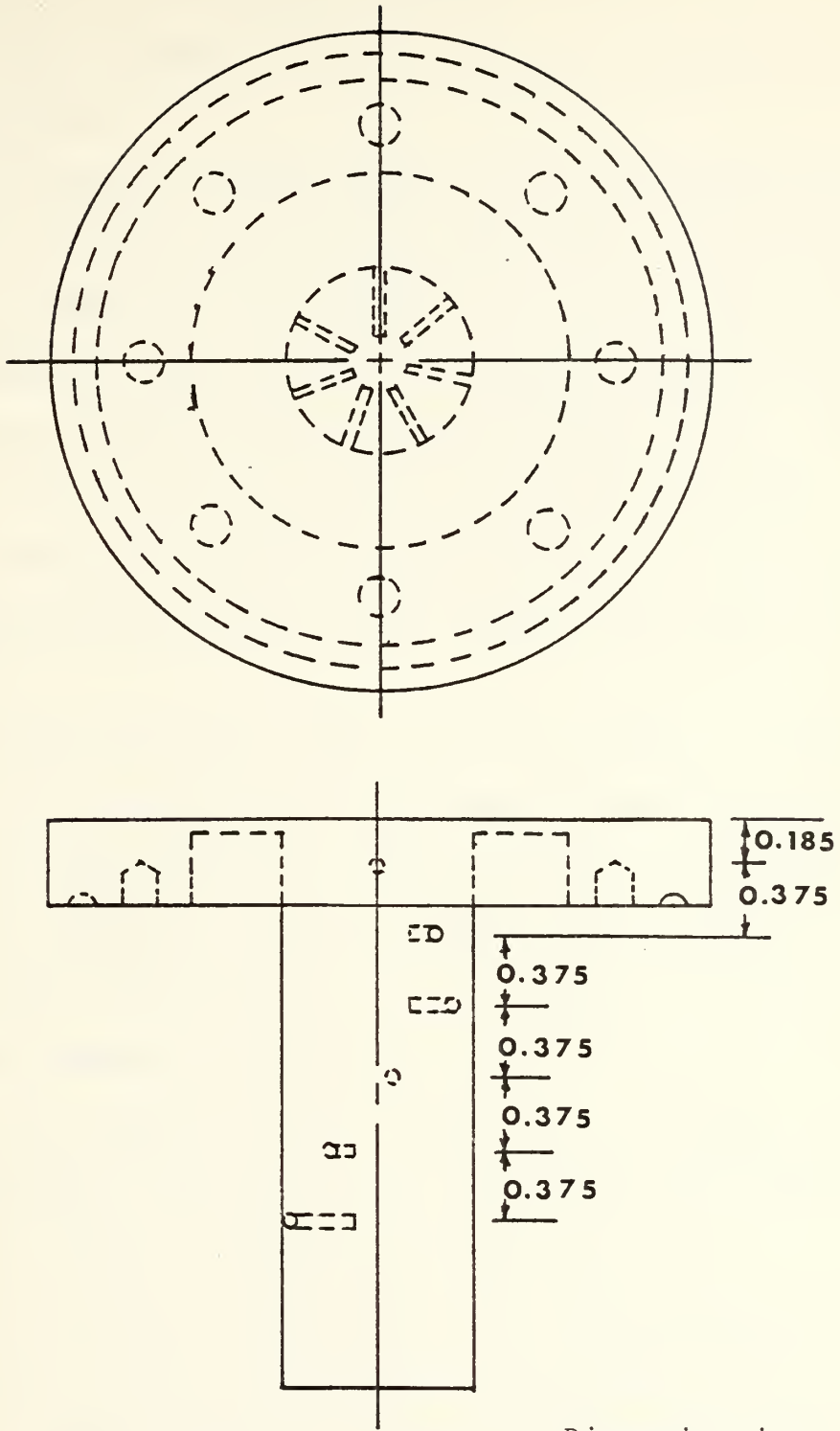

Figure 9. Test Surface Thermocouple Placement

the order of 0.010 inches (0.025 cm) thick, and a large external metal flange to allow securing of the surface in the test platform.

The choice of a test surface with a circumferential fin attached was based on problems with rogue nucleation experienced by previous investigators [9,10,11]. Previous designs utilizing only a cylindrical test section were all hampered by rogue nucleation sites around the edge of the test section. This spurious nucleation not only interfered with a clear viewing of the actual test surface but also prevented accurate determination of heat transfer from the test surface as well.

Chapman [8] solved this problem by using a T-shaped test section with the central core being a copper cylinder and the test surface being an extremely thin, brazed piece of type 304 austenitic stainless steel. This test section performed quite satisfactorily but presented a tremendously difficult surface to fabricate.

For the purposes of this experiment the same general idea of a T-shaped test section was utilized, but a decidedly simpler fabrication technique was developed.

The objective in producing a thin circumferentially finned test section was to enhance the performance of the test section. A continuous test surface of homogeneous material was chosen to suppress rogue nucleation problems and to reduce the measurement difficulties that arise when several different materials are used.

Coupled with the relatively poor conduction properties of type 304 stainless steel, the thin circumferential fin served the purpose of choking off the radial heat flow from the test surface. Throughout this experiment the fin worked extremely well. A finite element analysis of the test surface performed by Lt. Pete Harrell, USN, a graduate student in Mechanical Engineering at the Naval Postgraduate School, gave analytic verification of a one-dimensional temperature profile across the test surface. At no time during the experiment were any nucleation sites external to the one-inch core of the test surface ever observed.

The test surface was manufactured of the type 304 austinetic stainless steel to give a large axial temperature gradient, thereby enhancing the performance of the test surface as a heat flux meter. Six thermocouple wells were placed along the shaft nominally at a peripheral variation of 50 degrees with an axial spacing of 0.375 inches (0.953 cm), the top thermocouple being located at 0.1835 inches (0.466 cm) from the boiling surface. Each well was drilled to a nominal depth of 0.375 inches (0.953 cm) and a diameter of 0.040 inches (0.102 cm). The thermocouples used were Omega, 0.040 inches (0.102 cm) stainless steel sheathed, copper-constantan thermocouples, calibrated as indicated in Appendix A. Figure 10, a plot of the axial variation in temperature during representative test, is a graphical representation of the performance of the test surface as a heat flux meter. Clearly the large axial temperature variation offered by the stainless steel coupled with an accurate location of the thermocouple

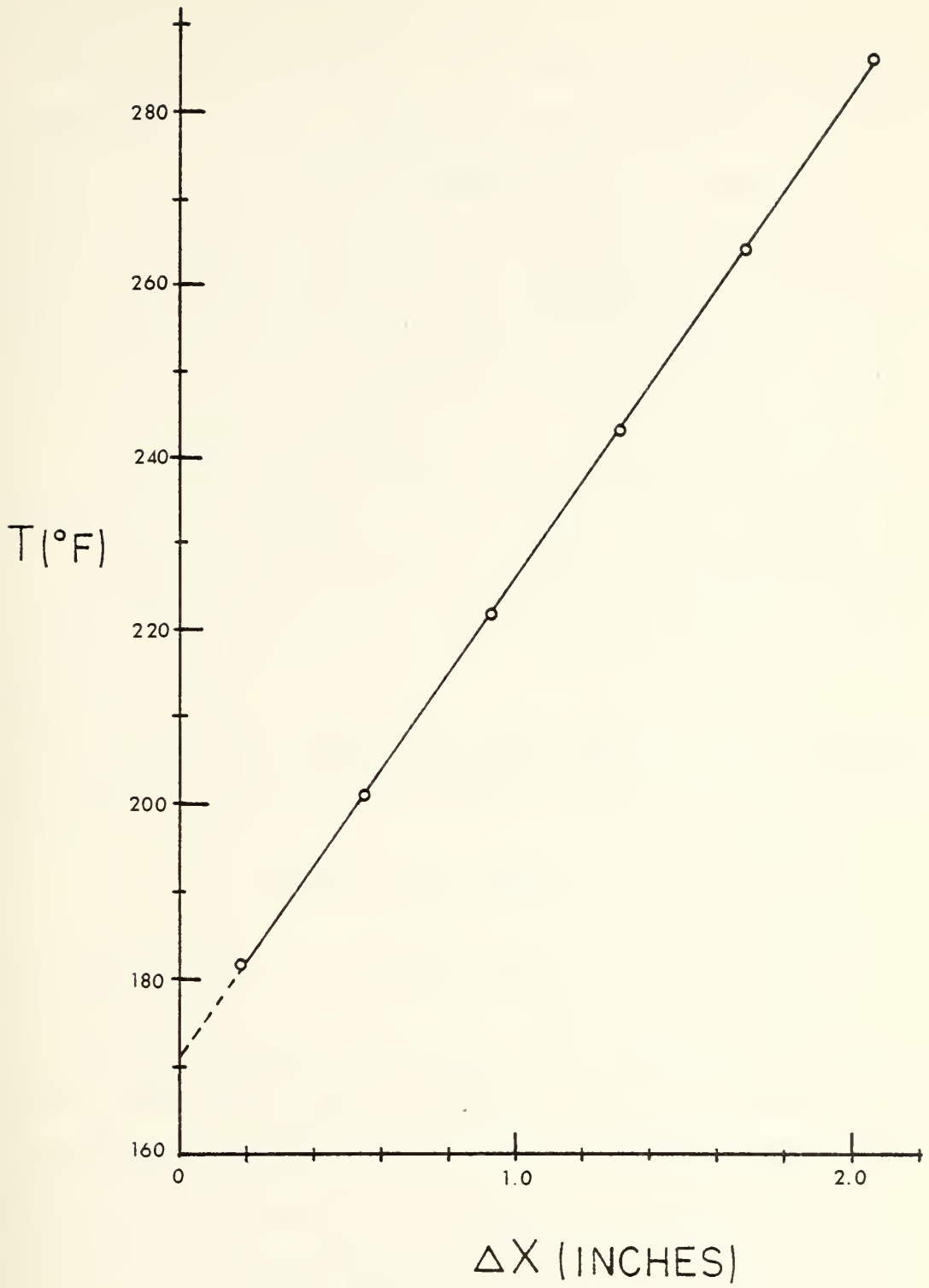

Figure 10. Axial Temperature Variation in the Test Surface

beads provides an excellent method for extrapolating the temperature of the boiling surface.

The surface temperature, Tw, used in the calculation of the superheat, ΔT_{sat}, was established through an extrapolating process. All of the thermocouple readings, TC1-6, for the test section were used in a polynomial regression to generate an extrapolated surface temperature. Additionally, an extrapolated surface temperature was established using only the two thermocouples closest to the boiling surface, TC5-6. The difference between these two extrapolated surface temperatures was generally on the order of two degrees F or less. The arithmetic average of these two extrapolated surface temperatures was taken, and the result was the surface temperature, Tw.

Once the surface temperature was established, the superheat, ΔT_{sat}, could be calculated in the following fashion:

$$\Delta T_{sat} = T_w - T_{sat}$$

where $T_{sat} = 117.6^{\circ}F$ ($47.56^{\circ}C$) [12]

The thermal conductivity, Kss, as a function of the test material temperature was calculated using the data for type 304 austenitic stainless steel from Touloukian [13]. The equation used throughout this experiment was:

$$K_{ss} = 9.36 + 0.0043\ (T_{ss}-200)$$

where Kss is in BTU/hr-ft $^{\circ}F$ and Tss represents the temperature, in degrees F, of the stainless steel test section

as computed from the arithmetic average of the temperature readings of the two thermocouples closest to the test surface, i.e.,

$$Tss = \frac{TC6 + TC5}{2}$$

where TC6 represents the temperature reading, in degrees F, of the thermocouple nearest the test surface and TC5 represents the temperature reading, in degrees F, of the thermocouple immediately below TC6.

Using the measured distance between the thermocouple beads of TC6 and TC5 to represent the variation in the axial direction, Δx, measured in feet, over which the temperature variation, ΔT, occurs, Fourier's Law of Heat Conduction can be used to calculate the heat flux in the test section. In general, Fourier's Law of Heat Conduction for a one-dimensional system is written as

$$q = -Kss \frac{dT}{dx}$$

where q represents the heat flux (Q/A)

Kss represents the thermal conductivity of the test surface material

$\frac{dT}{dx}$ represents the temperature gradient in the x direction

Substituting in the previously defined elements of Fourier's equation yields the following:

$$q = -Kss \frac{TC6 - TC5}{\Delta x}$$

In these experiments TC5 will always be larger than TC6; therefore, the heat flux, q, will always be positive.

The heat transfer coefficient, h, having the units of BTU/hr-ft^2 ^{o}F, can be found by a simple energy balance on the system. Using Newtons Law of Cooling, q = h(Tw - Tsat) an energy balance yields:

$$-Kss \frac{dT}{dx} = h\ (Tw - Tsat)$$

then

$$h = \frac{-Kss \frac{dT}{dx}}{(Tw-Tsat)}$$

which simplifies to:

$$h = \frac{q}{\Delta Tsat}$$

Appendix B contains a detailed analytic solution to the circumferential fin problem and the development of the correction factor that was applied to account for the heat loss through the fin.

B. TEST SURFACE FABRICATION

As previously discussed, the major difference between the test surface used in this experiment and the one used by Chapman [8] is that this one is manufactured from a single, homogeneous piece of material.

The key to fabrication of this type of surface lies in the use of a support jig, figure 11. By securing the test

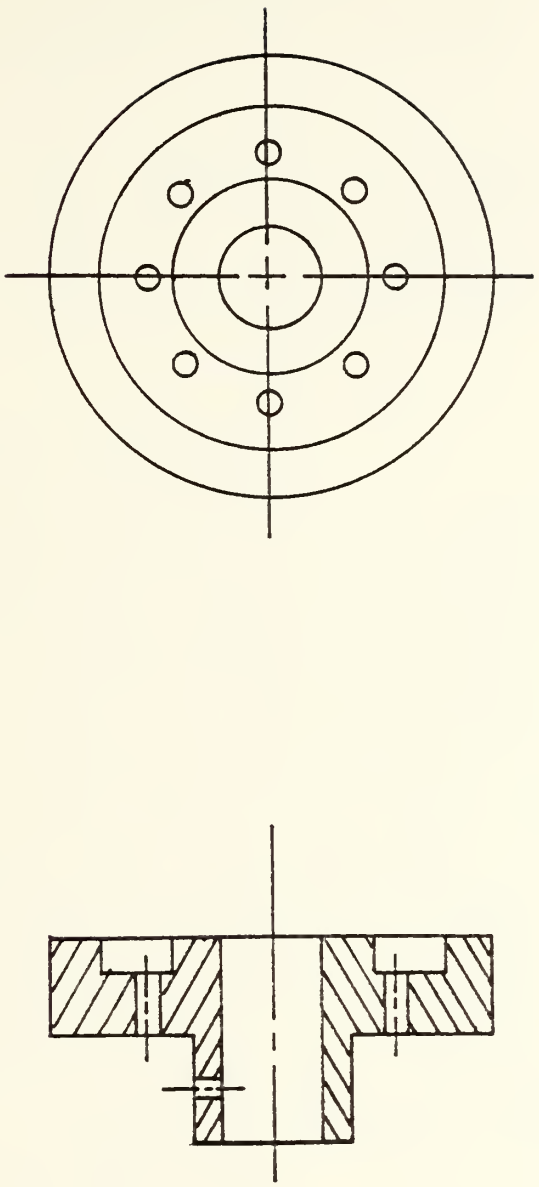

Figure 11. Test Surface Support Jig

surface in the support jig, final facing cuts could be taken on a lathe. The jig and test surface fit together in such a way as to form a body rigid enough to allow the boiling surface to be turned down to a fin thickness of approximately 0.010 inches (0.025 cm).

The test surface remained in the support jig throughout all stages of manufacture, being removed only for physical measurements of the test surface and prior to installation of the surface in the boiling tank.

C. METALLOGRAPHIC PROCEDURES

In an attempt to remove as many "natural" nucleation sites as possible, the surface was subjected to a rather extensive series of metallographic polishing steps. The surface was first hand lapped on a true plate with Buhler metallographic paper, starting with a 1/0 grit and then turning the surface 90 degrees and completing with 3/0 grit. The surface was then mechanically polished on a Buhler metallographic wheel using felt cloth impregnated with Metadi paste diamond grit and lubricated with alcohol. The surface was first polished with a 6 micron grit, then a 3 micron grit and finally a 1 micron grit wheel.

Upon completion of polishing, microscopic examination of the surface revealed a mirror finished surface virtually free of nucleation sites.

D. ARTIFICIAL CAVITIES

To investigate the effects of artificial nucleation sites on both convection heat transfer and the incipience of pool

boiling, various number and geometric arrangements of artificial cavities were drilled in the test surface. These cavities were formed by a tapered twist drill and were made to be 0.015 inches (0.038 cm) in diameter and 0.015 inches (0.038 cm) in length, the length being measured from the boiling surface to the shoulder on the taper as shown in figure 12.

As artificial cavities were added to the surface, the last three steps of the polishing process were briefly repeated to remove any burrs around the edge of each cavity. Figure 13 displays micrographs which indicate what the mirror finish surface condition was in comparison to the size of the artificial cavity.

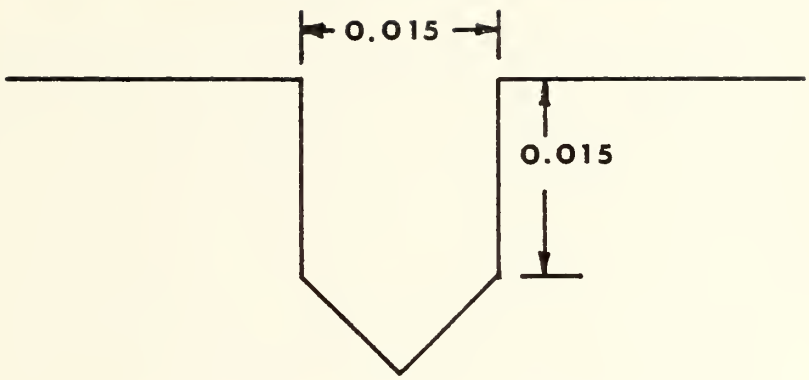

Dimension in
inches

Figure 12. Cross-Sectional View of a Single Artificial Cavity

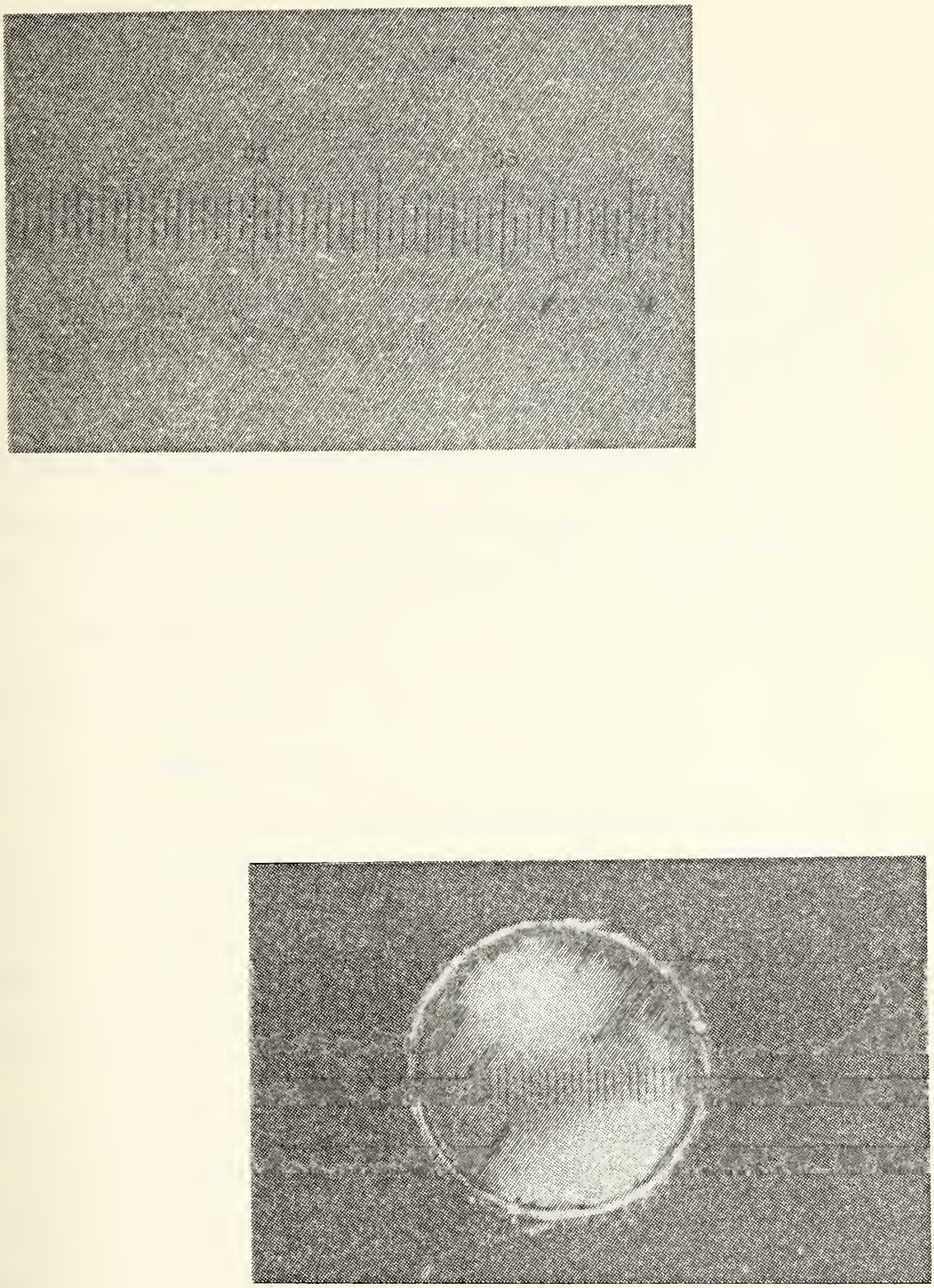

Figure 13. Comparison of Test Surface Finish to Artificial Cavity Size

III. EXPERIMENTAL PROCEDURE

A. TEST SURFACE PREPARATION

With the test surface appropriately polished as described in the previous section, the only preparation that remained was the proper cleaning of the surface. This was accomplished by bathing the surface in acetone and drying with both a blower and soft tissue paper. A visual inspection as to the cleanliness of the surface was made under a light microscope. This inspection procedure was especially important when the artificial cavities were present in the surface to ensure that all traces of the polishing compounds had been properly eliminated.

B. FLUID PREPARATION

The fluid used in this experiment was Freon 113 (trichlorotrifluoroethane). To insure a pure test fluid industrial grade, Freon 113 was distilled in a Pyrex standard laboratory distilling system. The fluid was collected in clean glass containers and then transferred to the boiling tank.

C. ARTIFICIAL CAVITY PLACEMENT

The surfaces used in this experiment were designed to conform with those used by Chapman [8] and Penkitti [13]. In particular the geometric arrangement and cavity diameters were similar to Penkitti's [10]. The test program entailed the testing of a blank test surface followed by one cavity,

seven cavity and 13 cavity test surfaces. Figures 14 through 16 show the placement of the cavities for the one, seven and 13 cavity surfaces respectively. All photographs in these figures were taken prior to use as a boiling surface.

In the case of the one cavity surface, the cavity was located as close as possible to the center of the test surface. The additional cavities were added in groups of six, with each cavity at a peripheral spacing of 60 degrees. The additional groups of cavities formed concentric rings equally spaced in the radial direction. The first group of six cavities was placed on a radius of 0.125 inches (0.317 cm), and the second group of six cavities was placed on a radius of 0.250 inches (0.635 cm).

D. TEST PROCEDURE

The concept of the tests conducted in this experiment was to start with the test section and fluid at ambient temperature, raise the temperature of the fluid to its saturation temperature (117.6 F) and then through regulated incremental changes in input power to the test surface heater block take thermocouple and input power data when steady state was achieved.

Data were taken in two different directions (i.e. increasing and decreasing temperatures) during this experiment. This was done for two reasons, the first of which was to check for any hysteresis effects in the apparatus while the second, and perhaps most important, reason was to model work previously completed by Chapman [8], Penkitti [10] and Corty and Foust

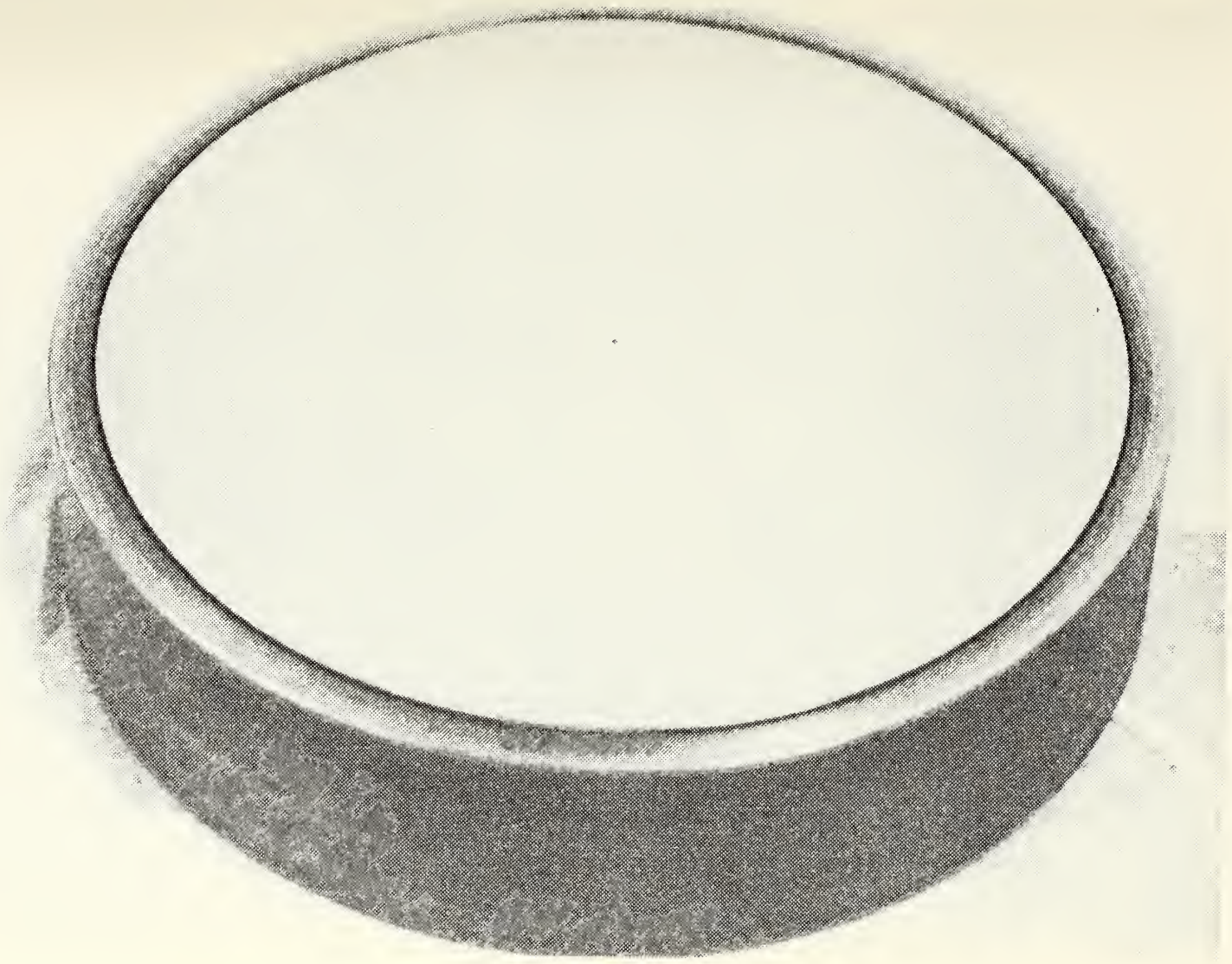

Figure 14. One Cavity Surface before Test

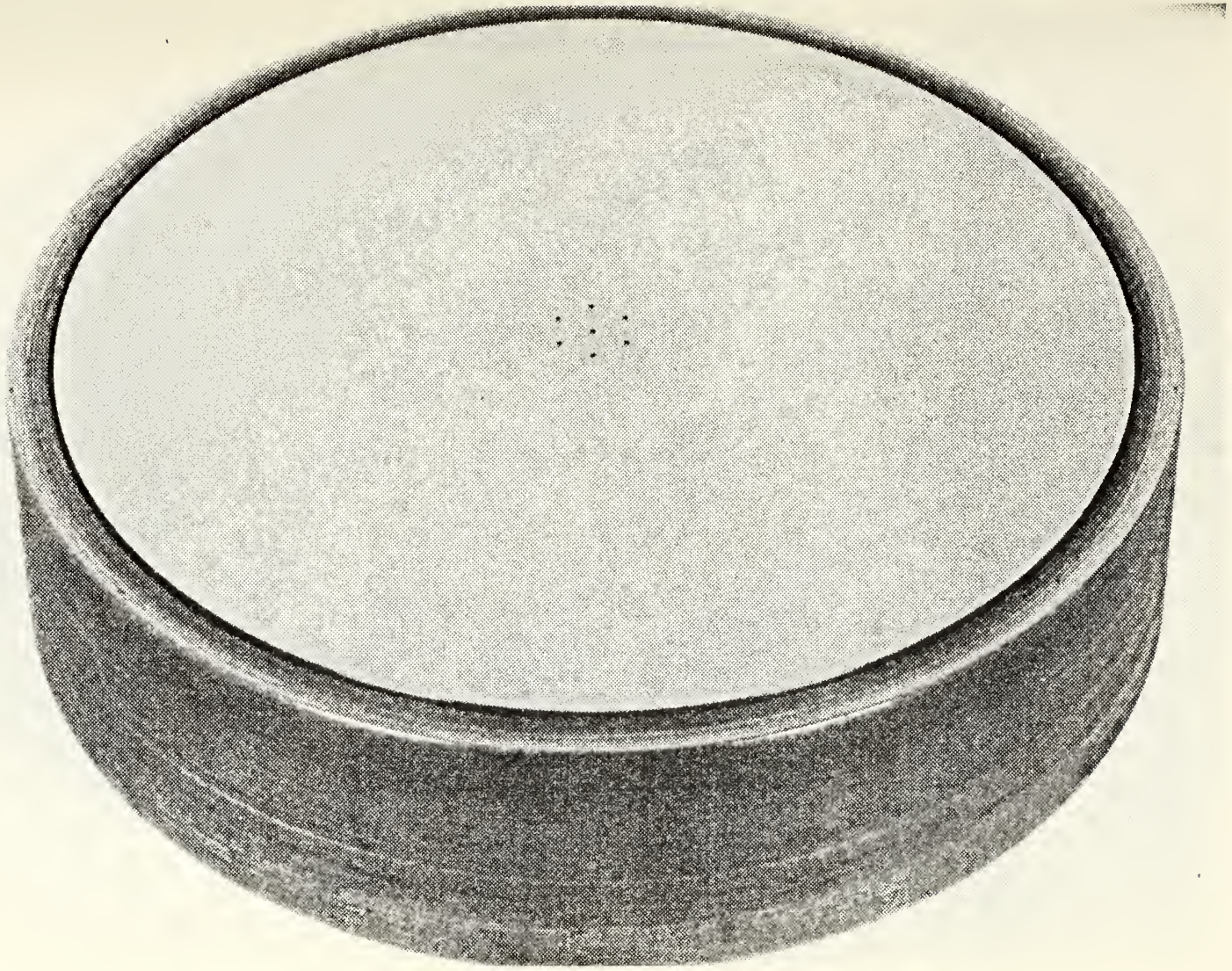

Figure 15. Seven Cavity Surface before Test

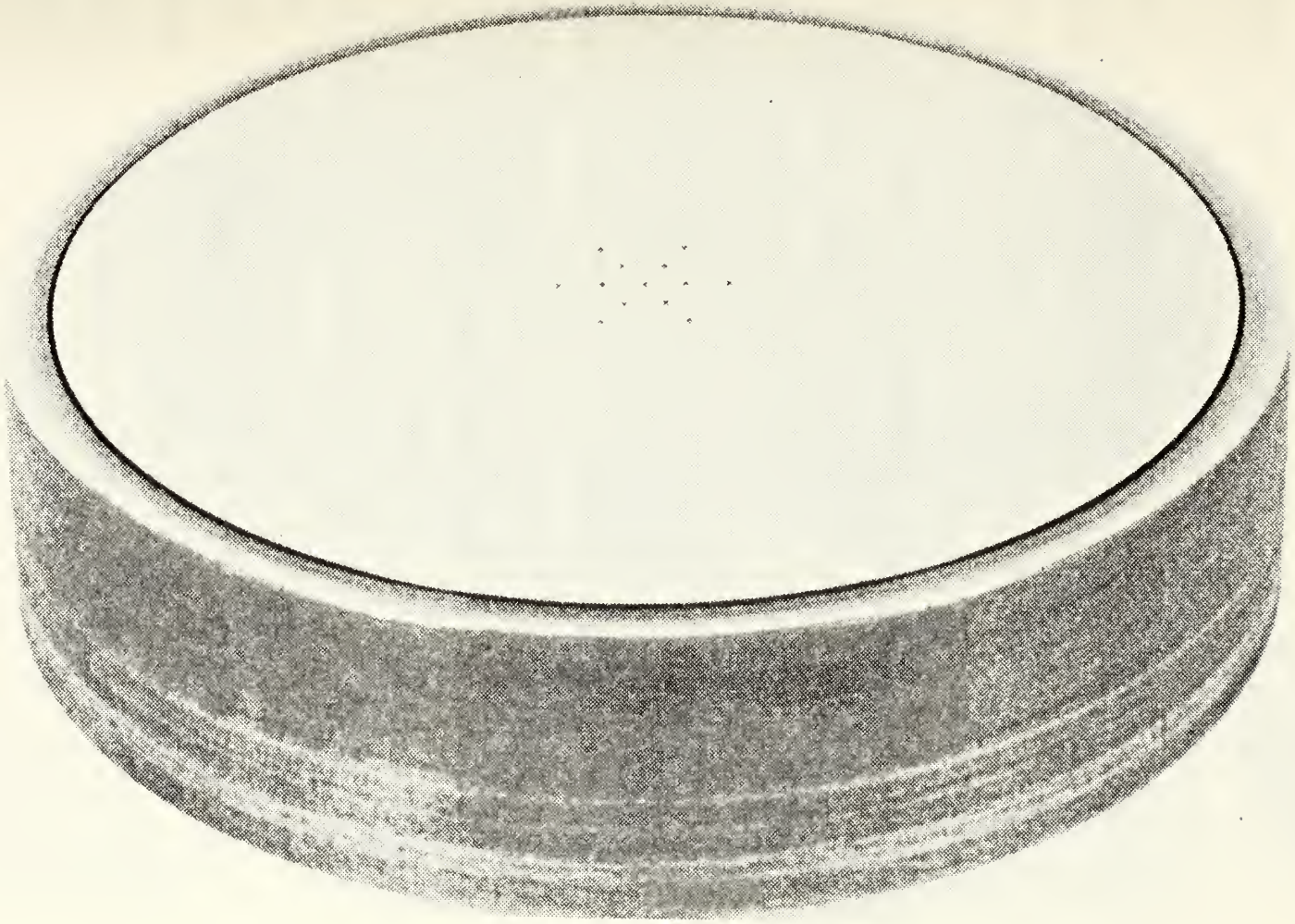

Figure 16. Thirteen Cavity Surface before Test

[4]. Due to the differences caused by the superheat condition and the activation/deactivation of nucleation sites, the taking of data for the two separate cases (temperature increasing and temperature decreasing) constitutes the running of two completely different experiments.

In the case of the temperature increasing situation, the test section and the fluid are heated from the ambient room temperature to the saturation temperature of the fluid, at which point the data taking begins. The fluid temperature, through the use of the bulk heater, is maintained as close to its saturation temperature as possible while the temperature of the test surface is slowly raised through the natural convection region to the incipience of boiling and continuing on well into the saturated pool boiling region. This procedure entails the heating of the test fluid when there is a large superheat condition and when the nucleation sites are activating, a situation similar to the experiments of Penkitti [10] and Corty and Foust [4].

In the case of the temperature decreasing, the fluid is starting from a situation of maximum power into the test surface and an already well developed and violent boiling condition. The temperature of the test surface is continually reduced until it is approximately equal to the saturated temperature of the fluid. Conducting the test in this fashion allows data to be taken as the nucleation sites deactivate, an experimental situation similar to that of Penkitti [10] and Chapman [8].

The initial data run consisted of using a blank test surface (no artificial cavities present). This first data run was peculiar in that in addition to producing usable experimental data it also supplied answers to such questions as what time span was required to reach steady state for this particular apparatus and what type of behavior was to be expected from the surface. Consequently the first run was considerably longer than any of the subsequent trials due solely to the larger number of data points taken. The original procedure was to increase the input power to the test surface block heater by increments of approximately 0.5 watts and then take data readings every 30 minutes until it was felt that a steady state condition existed. Throughout this experiment steady state was defined to be a change in all thermocouple readings of 0.5 F (0.28 C) or less in a 15 minute time period. After taking the first few data points it became clear that the operating characteristics of the test surface were such that steady state conditions were essentially reached after a period of four hours. Once this characteristic was established, the operating procedure became one of changing the input power setting to the test surface heater block and then returning after a period of three and one half hours to monitor the thermocouples and power settings at intervals of 15 minutes until a steady state condition clearly existed.

During the initial run 38 readings were taken while the temperature was increasing, and 15 were taken while the

temperature was decreasing. After plotting and evaluating this first experimental run it became clear that the phenomenon being observed could easily be analyzed with only a third of the number of data points taken for run number one. Therefore, on data runs 2-6 there were a total of 21 points taken for every surface, 11 with the temperature increasing and 10 with the temperature decreasing.

E. BULK HEATER OPERATION

Throughout this experiment a concerted effort was made to maintain the temperature of the fluid at its saturation temperature. As mentioned previously and as shown in figure 6, a Nichrome wire resistance heater connected to a Variac formed the bulk heater system. The temperature in the fluid tank was measured by two independent sources. One was a copper-constantan thermocouple located directly above the center of the test surface at a distance of approximately 0.250 inches (0.635 cm). The other was a set of eight copper-constantan thermocouples, connected in series, and placed in pairs located peripherally at 90 degree intervals around the tank. Of the two members of each pair, one thermocouple was located near the top of the tank, and one was located near the bottom. This connection of eight thermocouples was placed in a ring outside the boundary of the test surface. Since these thermocouples were connected in series, they gave a single average bulk temperature of the fluid.

The procedure followed during the experiment was to set a power level into both the bulk heater and the test surface and then wait for the steady state conditions. To minimize the interference of convection cells or circulation patterns that developed from the bulk heater, the heater was always turned off prior to taking the actual data points of record. This would occur when the stainless steel test surface showed that it met the established steady state criterion set forth for the experiment, generally one-half hour prior to the taking of the actual data point.

As the experiment progressed, the increased temperature of the test surface contributed more and more to keeping the fluid temperature at its saturation temperature. This, of course, meant that as the input power to the test surface increased, the input power to the fluid bulk heater would decrease. This procedure continued for the first five or six data points at which time use of the fluid bulk heater could be completely disregarded. From this point the temperature of the test surface itself was sufficient to maintain the fluid temperature at the proper level.

The procedure for the situation in which the temperature was constantly decreasing was exactly the opposite of the previously described procedure, i.e. the fluid bulk heater was not used until the last few points were reached.

F. GLASS CYLINDER

A careful examination of figure 6 will reveal a cylindrical section of glass located on top of the test surface.

This portion of the test apparatus is a modification to the original arrangement.

The purpose of the glass cylinder was to minimize any circulation effects produced by the bulk heater in the fluid. It was felt that unless this type of circulation pattern were reduced, there would be little hope for seeing any influence of the artificial cavities in the natural convection heat transfer region. It was decided that a glass cylinder around the test surface would significantly reduce the fluid circulation from the outer regions of the fluid tank, restricting the actual area of investigation to that region of greatest interest, the surface of the test surface core, the test surface fin and the fluid directly above the test surface. Additionally, this modification helped maintain the geometric similarity between this experiment and that of Chapman [8]. The D/d ratio of the glass section used in this experiment, where D represents the inside diameter of the glass cylinder and d represents the diameter of the test surface central core, was set at 3.125, which compares favorably with that used by Chapman [8] which was 3.070.

IV. TEST RESULTS

During the course of this study a total of five different test surface configurations were examined. Data were collected for the following cases:

(1) Blank mirror finished surface without glass cylinder

(2) Blank mirror finished surface with glass cylinder

(3) Single cavity surface with glass cylinder

(4) Seven cavity surface with glass cylinder

(5) Thirteen cavity surface with glass cylinder

Two separate test surfaces were used, however, to help reduce the uncertainties that arise for surface irregularities in boiling studies, the data were identified by the nomenclature TS1 and TS2 which stand for test surface one and test surface two respectively.

1. Reproducibility

In an effort to gain an understanding of the characteristics and reproducibility of the test apparatus, TS1 was used in the first two test situations. The data for these experiments are presented in figures 17 and 18. Figure 17 is a representation of data taken with TS1 in the blank, mirror finished condition with the temperature of the surface increasing. It is a comparison of data for the cases in which (1) there is no glass cylinder present and the fluid bulk heater is left on during the taking of data and (2)

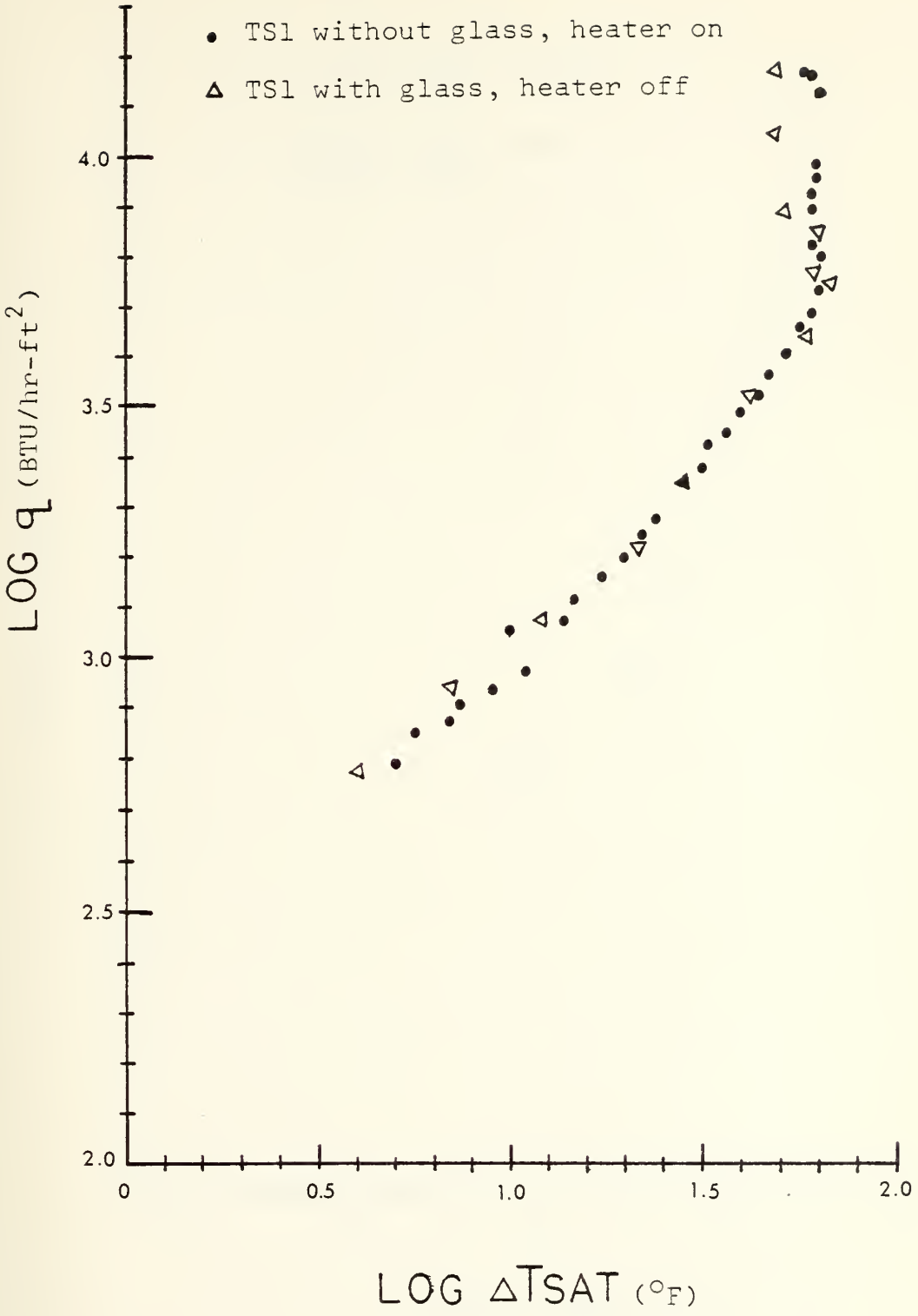

Figure 17. Comparison of TS1 with and without Glass and Heater, Temperature Increasing

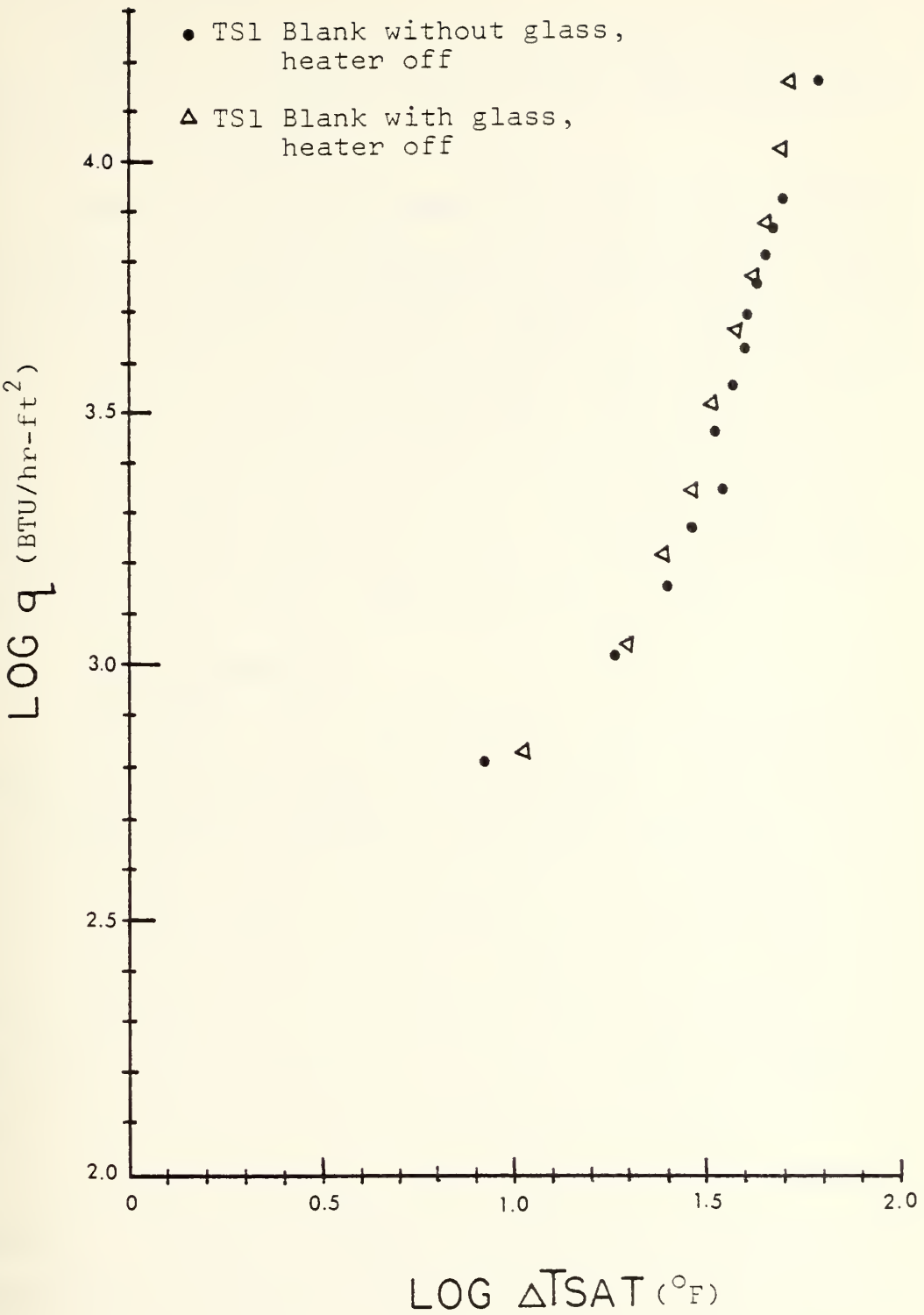

Figure 18. Comparison of TS1 with and without Glass and Heater, Temperature Decreasing

there is a glass cylinder and the fluid bulk heater is turned off prior to taking data.

Figure 18 represents the same surface both with and without the glass cylinder and with the fluid bulk heater off prior to taking data.

These two figures clearly show that the apparatus gave highly reproducible results. In addition this particular test demonstrated that the effects of convective circulation generated by the fluid bulk heater were insignificant in comparison to the circulation developed by the test surface. Irrespective of this all remaining tests were conducted with the glass cylinder in place and the fluid bulk heater off for the collection of all data.

2. Flow Circulation

Throughout this experiment a very strong and well developed circulation pattern was observed. This circulation was characterized by extremely vigorous convection currents across the test surface resulting in a well developed central plume directly over the one inch central core of the test surface, figure 19. The observed fluid circulation in this experiment was very similar to that observed by Sparrow and Husar [14] in their flow visualization studies.

As each individual test progressed, the incremental increases in the test surface temperature brought about a corresponding increase in the intensity of the circulation. This condition acted to form a very strong convection pumping action on the fluid.

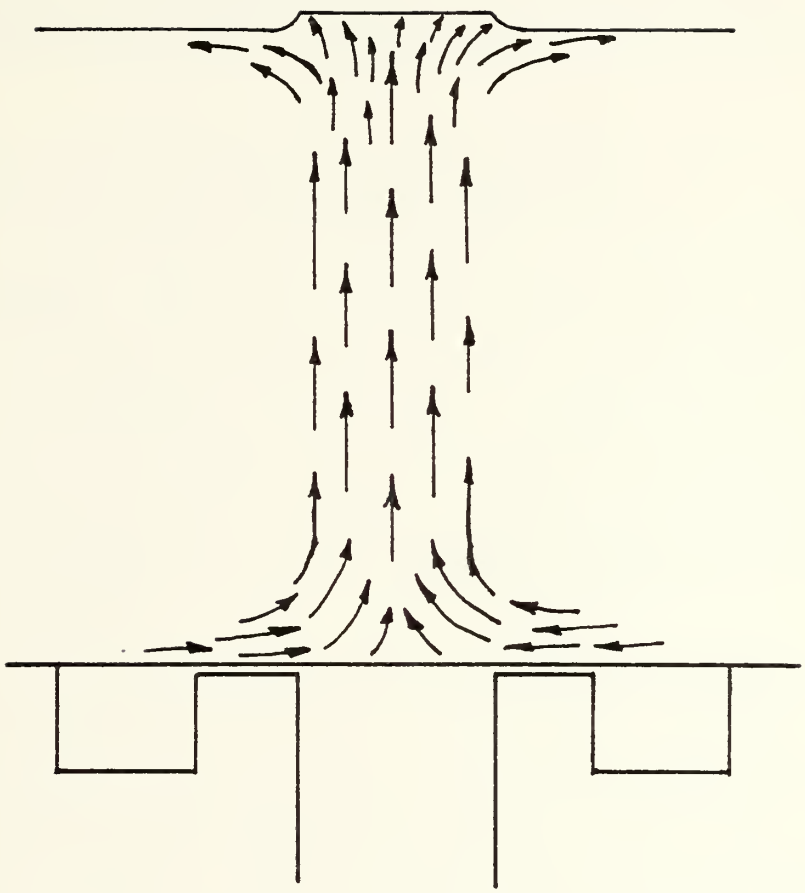

Figure 19. Fluid Circulation Pattern

Once the inception of nucleation occurred, nucleation sites activated rapidly with further increases in the heat flux. Observation of the fluid circulation at the highest heat flux revealed a violent boiling situation with large numbers of active nucleation sites on the one-inch central core of the test surface. As the bubbles left the surface, coalescence was observed as they rose through the fluid.

3. Test Surface Appearance after Use

At the conclusion of each test, the fluid was drained from the boiling tank, and the test surface was inspected for cavitation or erosion damage from the boiling process. In every test situation, after the test surface was allowed to dry, all surfaces were observed to have a white deposit on the one-inch central core of the test surface as illustrated in figures 20-23.

This deposit did not occur over the entire surface and seemed only to form at the location of active nucleation sites. A similar phenomenon was observed by Nail, Vachon and Morehouse [15] in their investigation of pool boiling nucleation sites on a type 304 austenitic stainless steel surface. In their experiment the test fluid was distilled water, and it was felt that the deposits were due to silica. No chemical analysis was made of the deposits observed in either this experiment or those conducted by Nail, Vachon and Morehouse [15]. It is considered interesting, however, that a similar phenomenon was observed in two separate experiments

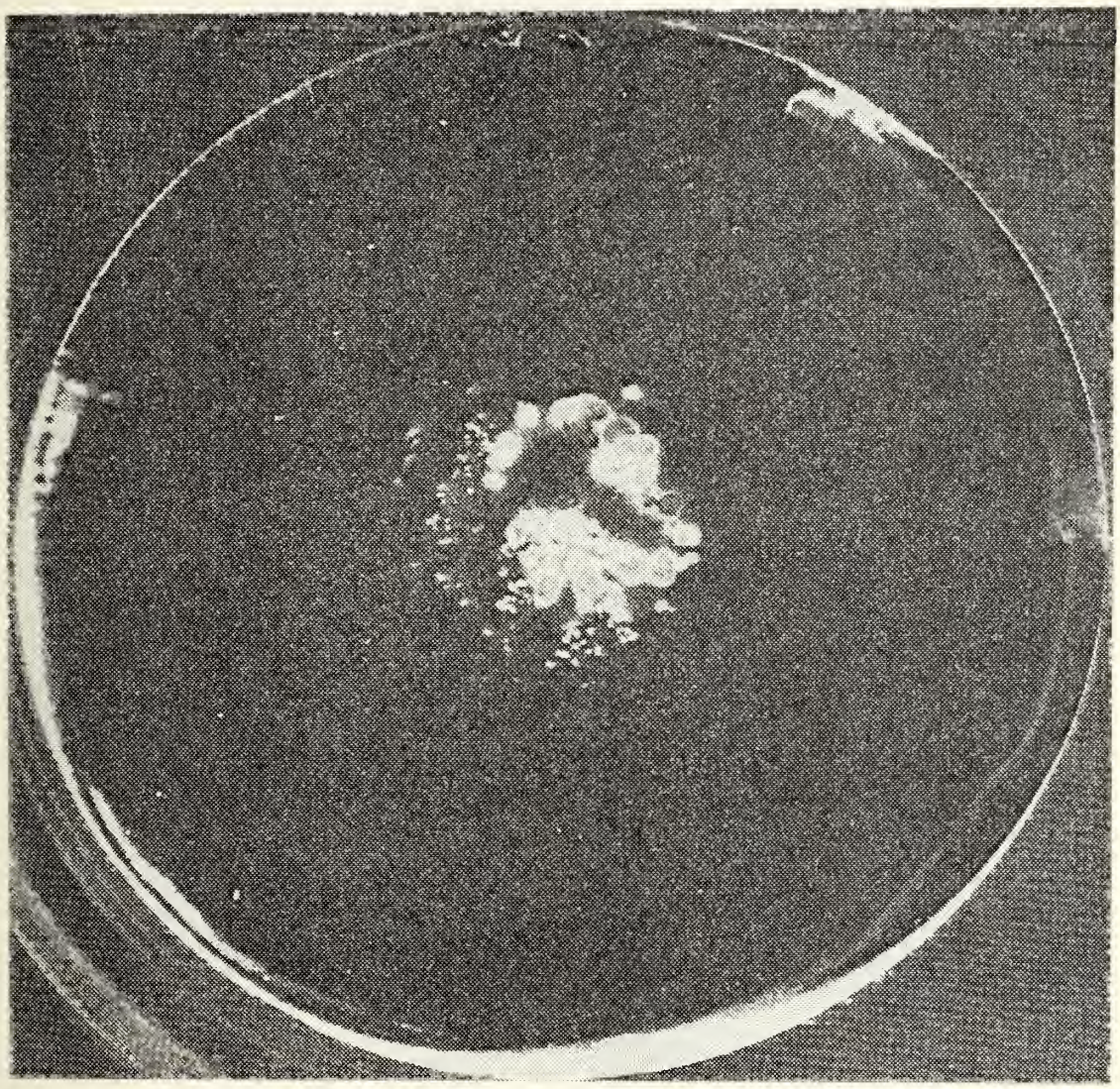

Figure 20. Blank Surface after Use

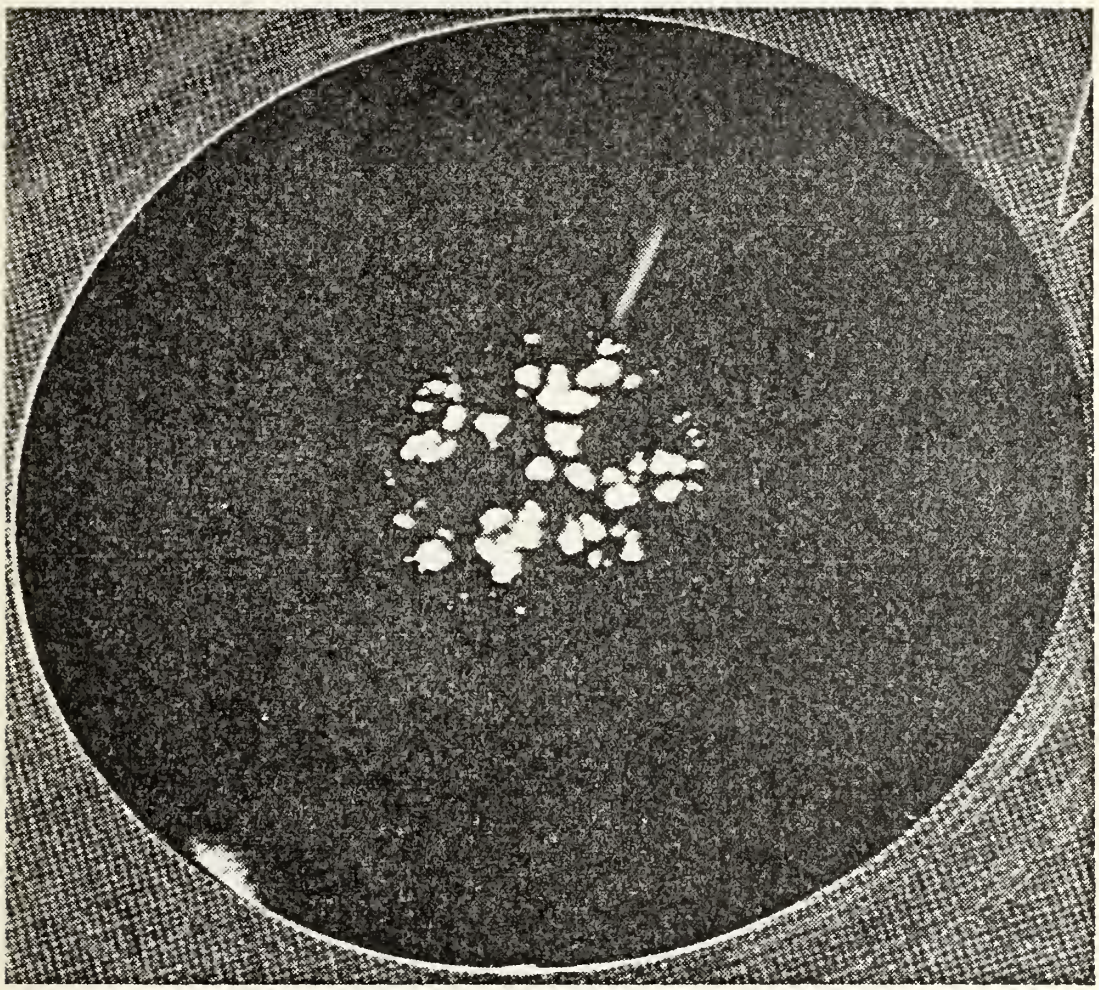

Figure 21. One Cavity Surface after Use

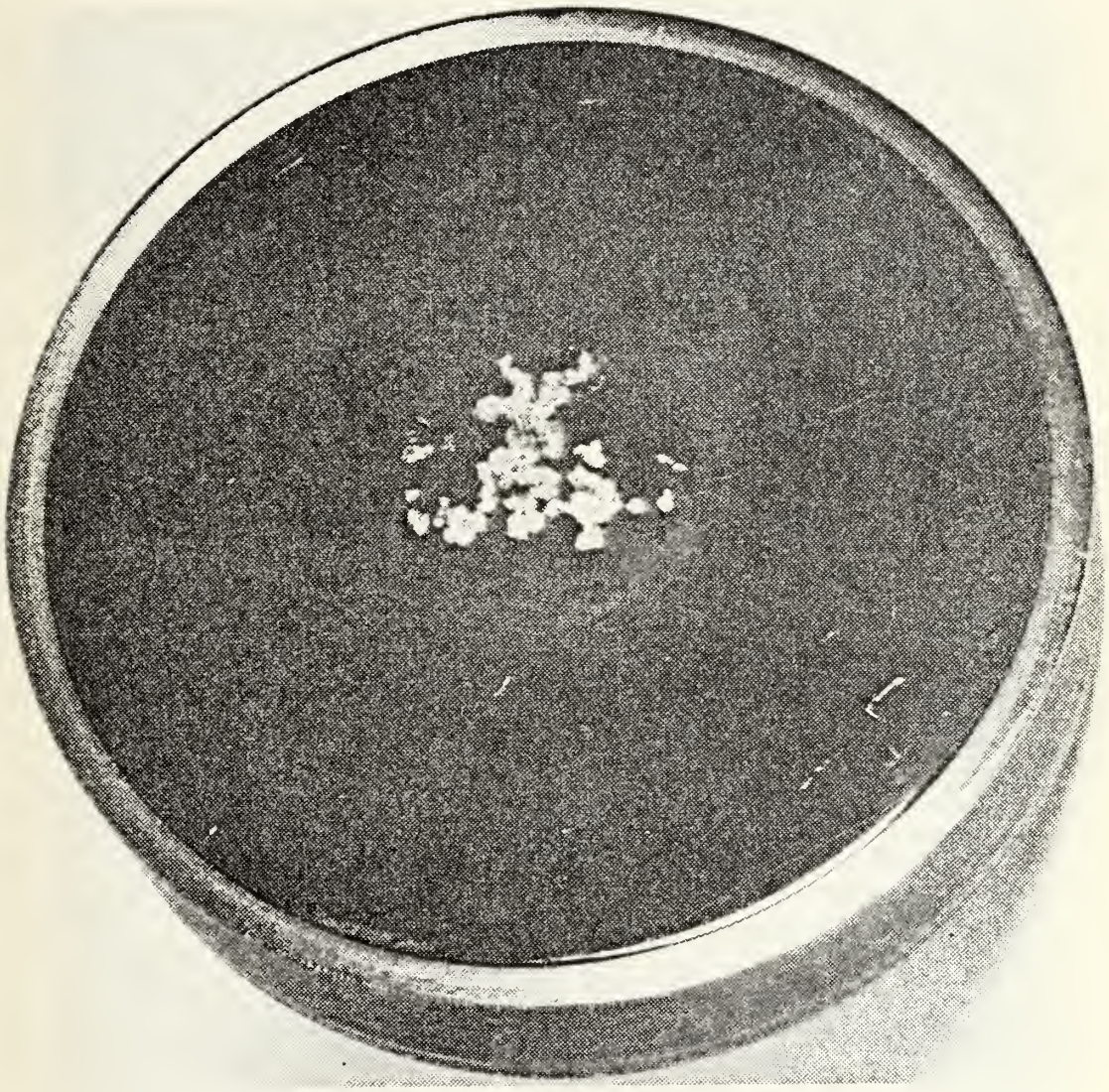

Figure 22. Seven Cavity Surface after Use

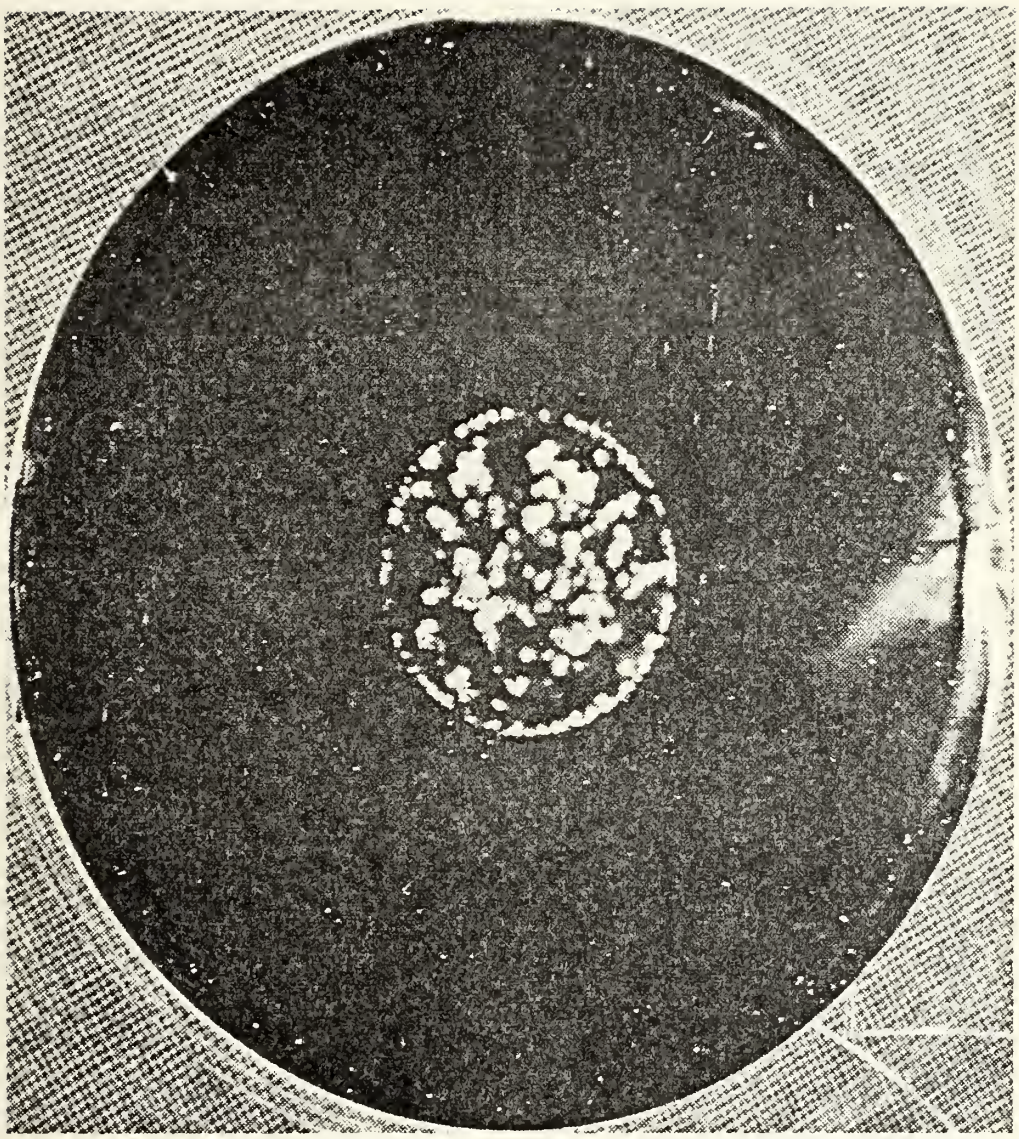

Figure 23. Thirteen Cavity Surface after Use

both using the same test surface material but totally different test fluids (distilled Freon 113 and distilled water). This seems to suggest the possibility that the deposits are a property of the test surface material.

Cleaning of the test surface with acetone and soft tissue was sufficient to remove all traces of the deposit. Visual inspection of the surfaces with a light microscope revealed no damage to any test surface as a result of the boiling process.

4. Test Surface Performance

Visual observation of the test surface in operation during the experiment gave every indication that the heat transfer surface was working very well. In the region of natural convection a circulation plume formed directly over the one-inch central core of the test surface and increased in intensity as the temperature of the surface was increased. The incipience of boiling was always observed to occur on the one-inch central core of the test surface which was exactly what was desired. As the heat flux into the test surface was increased the number of nucleation sites increased and were, at all times during the test, confined to the one-inch central core of the test surface.

The analytical evaluation of the test surface (Appendix B) served to illustrate that the performance of the test surface varied greatly depending upon the region of heat transfer being investigated, i.e. natural convection or nucleate boiling.

In the natural convection region, the losses in the heat transfer rate through the fin were up to 44 percent of the available heat transfer rate into the test surface. This situation steadily improves as the experiment progresses through the natural convection region and into the nucleate boiling region. At the point of highest input heat transfer rate, the losses through the fin drop to something on the order of 13.5 percent.

As demonstrated in Appendix B, the analysis in the natural convection region is quite sensitive to the convection heat transfer coefficient in the area over the fin. A major shortcoming of this experiment was the failure to instrument the test surface in such a way that the convection heat transfer coefficient over the fin could be experimentally determined.

It is worthwhile to point out, however, that since the solution to a circumferential fin type problem that exists with the geometry of this experiment is parametric in h, one should be very wary of the artificiality of the results from computer codes that solve this problem by an arbitrary choice of the convection heat transfer coefficient over the fin. The problem degenerates to one that is self fulfilling, i.e. pick an h and make the desired result.

Based on the analytically determined losses developed in Appendix B, the experimental data were corrected and plotted as displayed in figures 24-30.

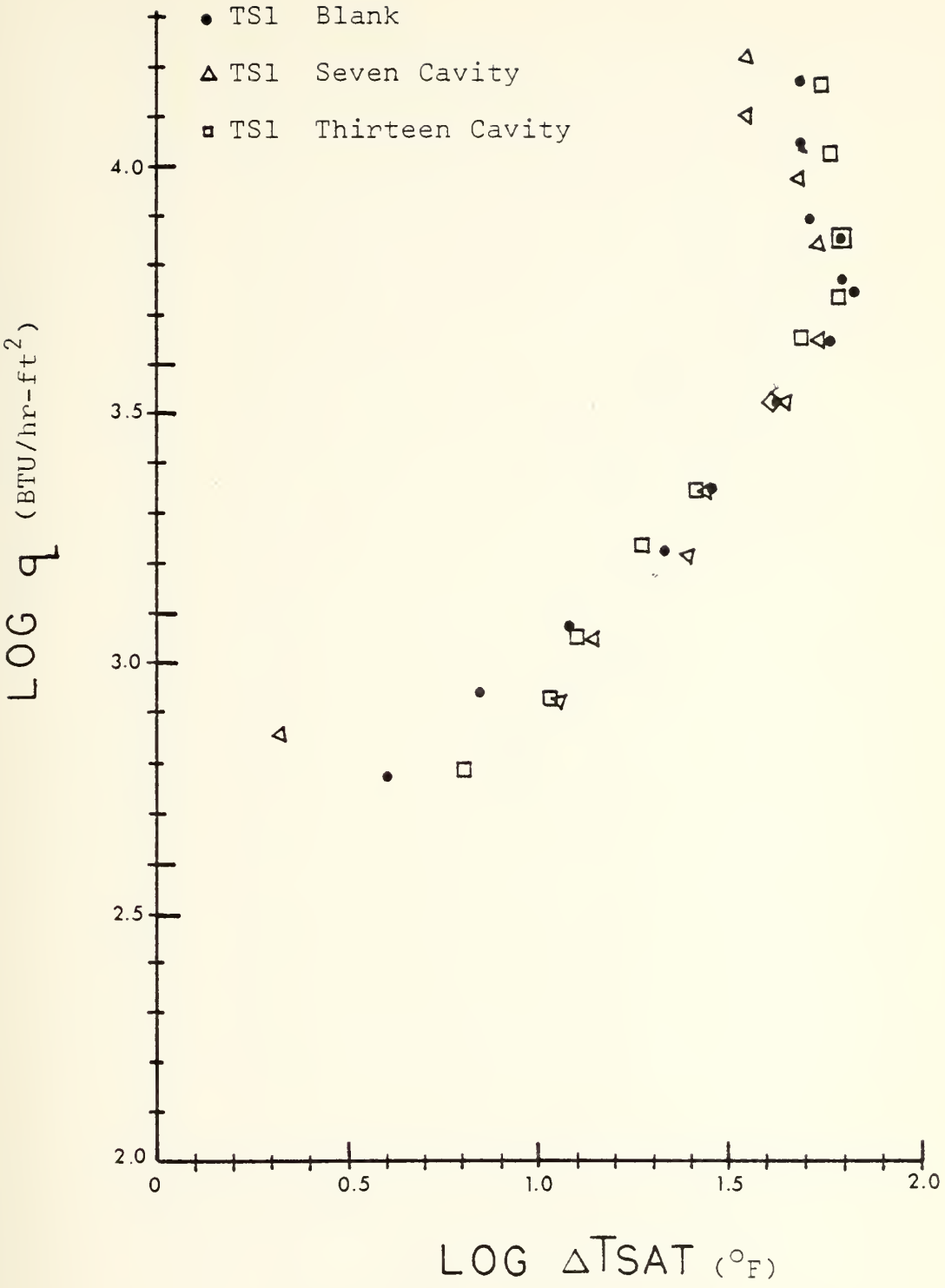

Figure 24. q vs. ΔTsat of Blank, 7 and 13 Cavity Surfaces, Temperature Increasing

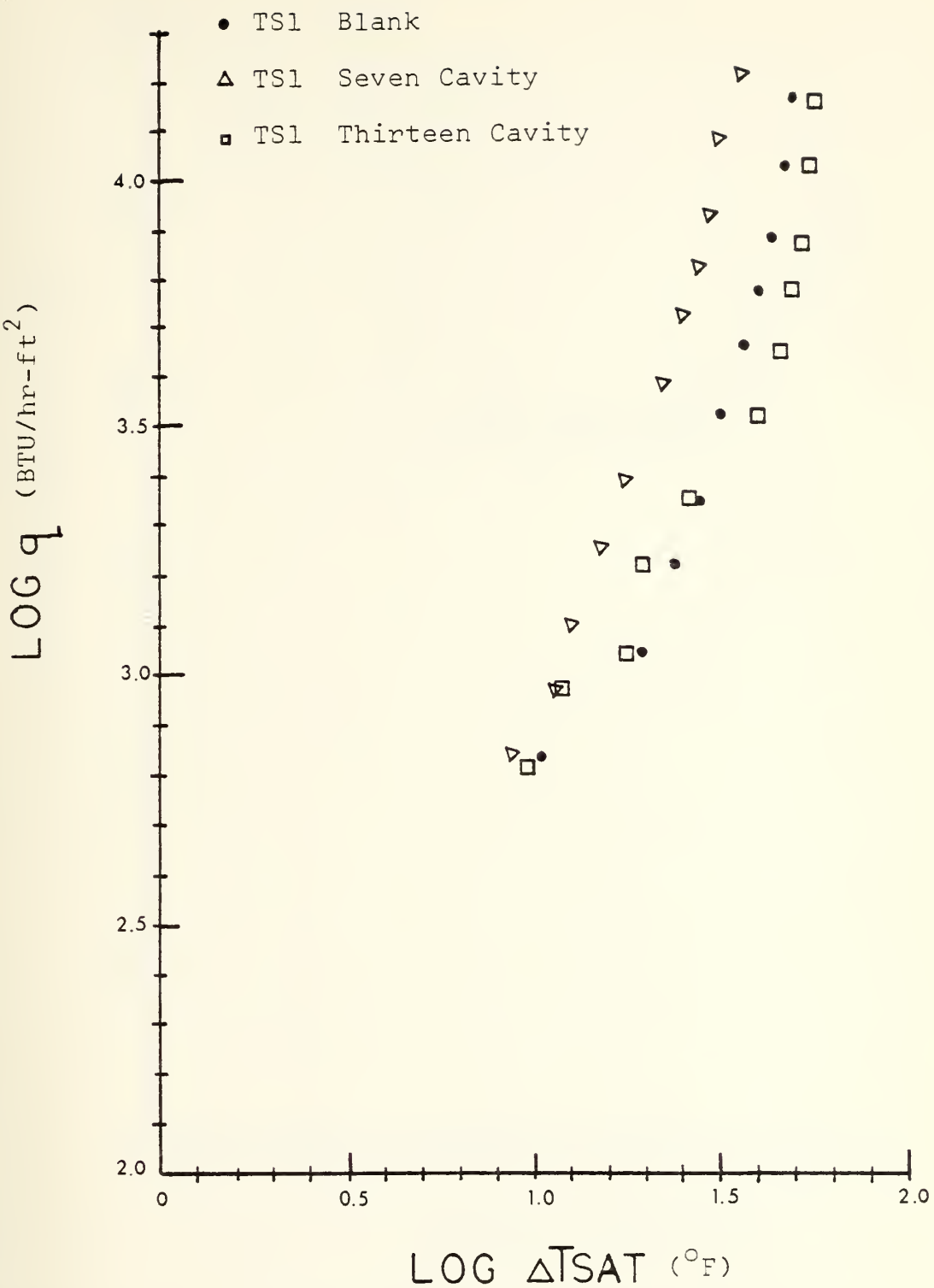

Figure 25. q vs. ΔTsat of Blank, 7 and 13 Cavity Surfaces, Temperature Decreasing

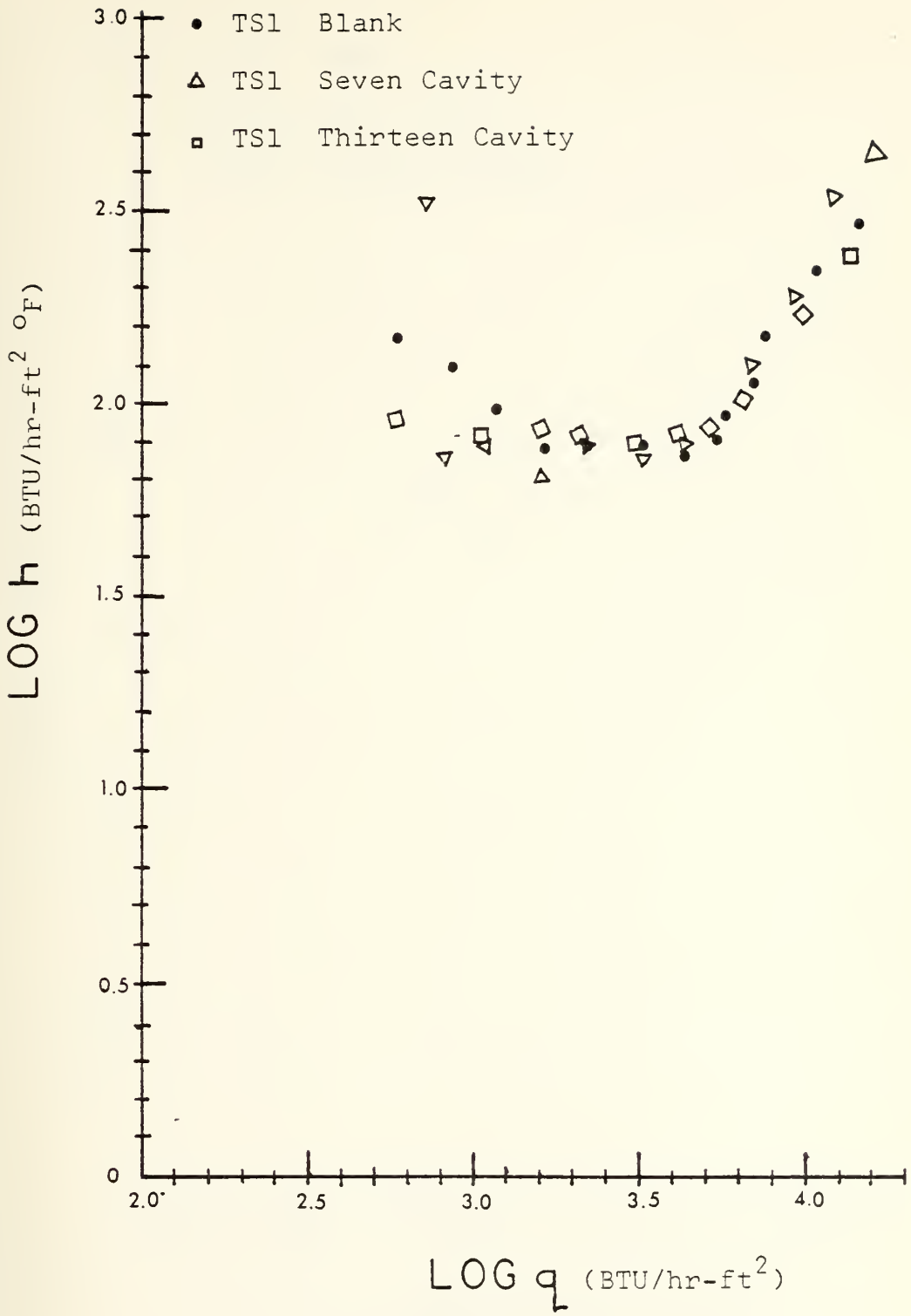

Figure 26. h vs. q of Blank, 7 and 13 Cavity Surfaces, Temperature Increasing

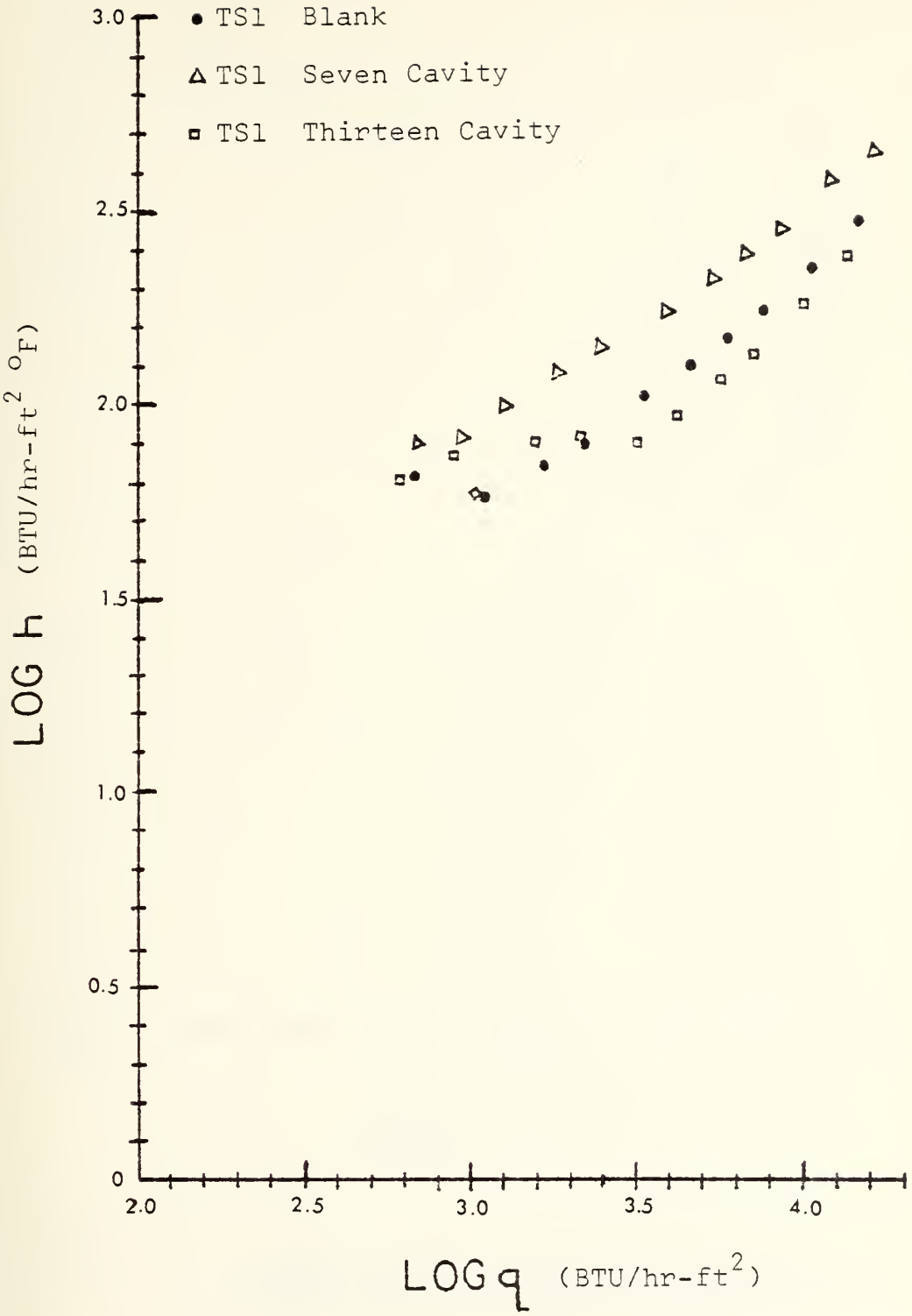

Figure 27. h vs. q of Blank, 7 and 13 Cavity Surfaces, Temperature Decreasing

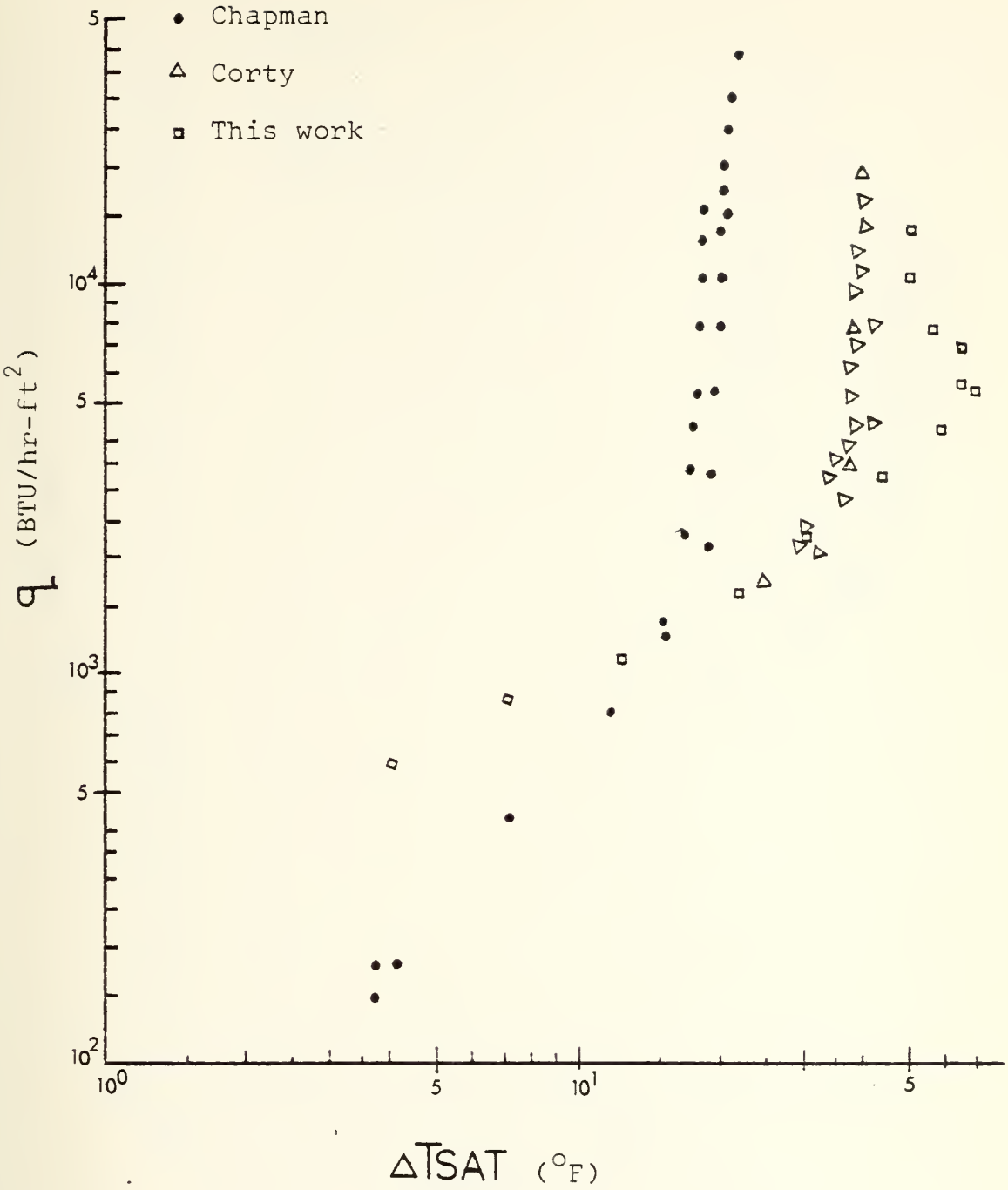

Figure 28. Comparison of Chapman's and Corty's Freon 113 Data with Data Obtained in this Work, Temperature Increasing

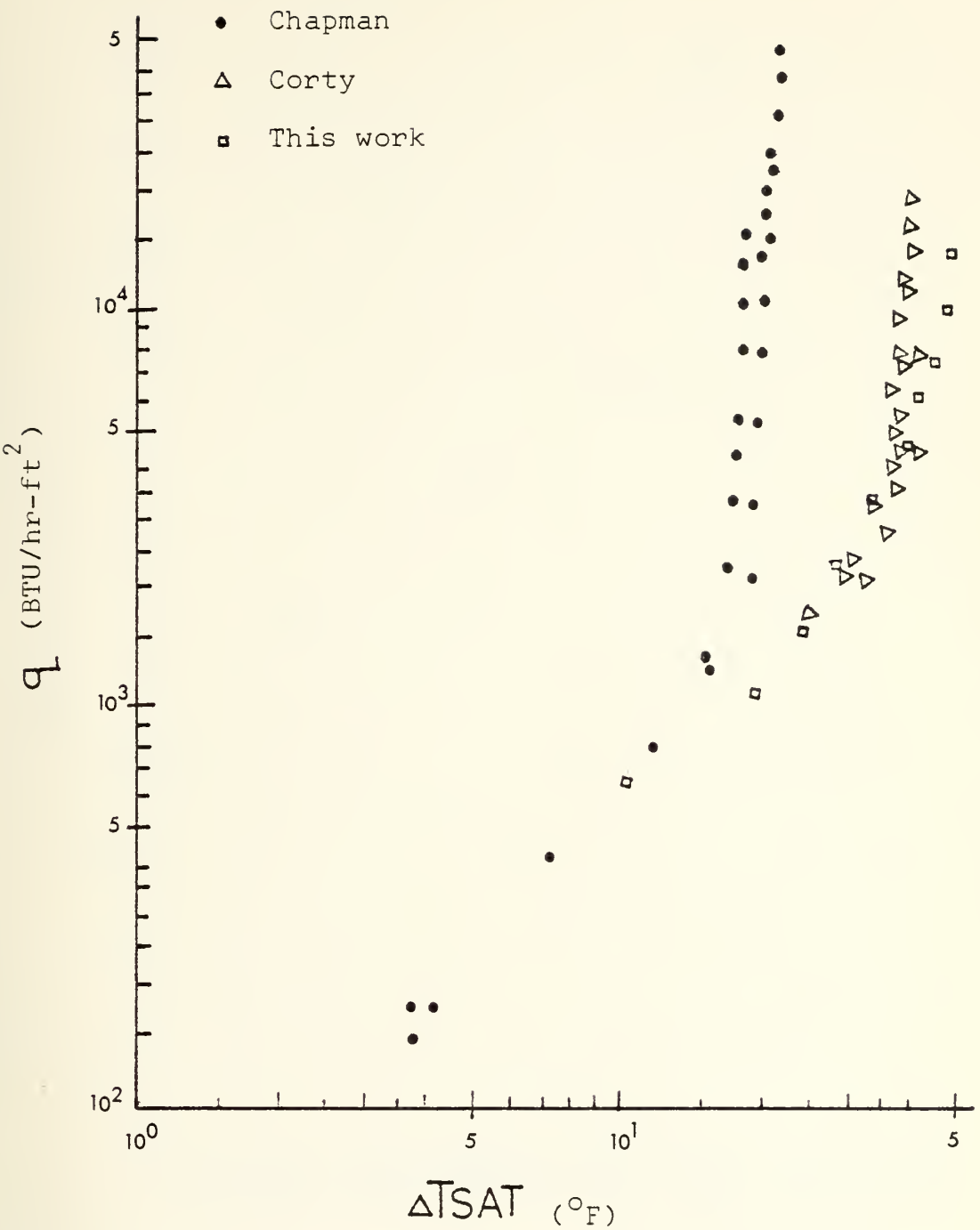

Figure 29. Comparison of Chapman's and Corty's Freon 113 Data with Data Obtained in this Work, Temperature Decreasing

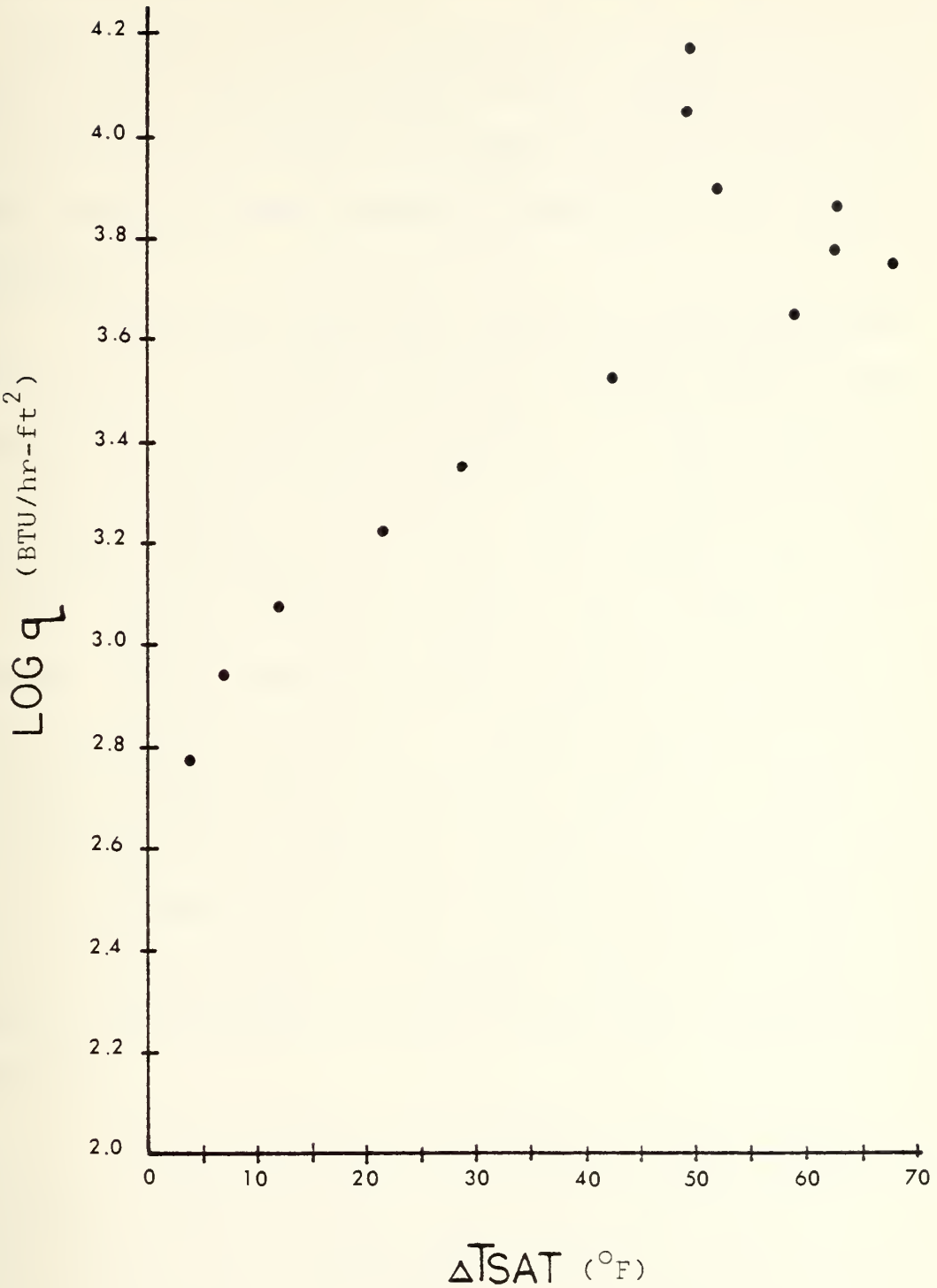

Figure 30. Observed Metastable Superheat, TS1 Blank

As can be seen from the graphical results of this experiment, there was, in fact, an improvement in the rate of heat transfer due to the presence of the artificial cavities for the case of the seven cavity surface. The failure of the 13 cavity surface to perform any differently than the blank mirror finished surface is proposed to be due to the following:

For every artificial cavity of a given diameter there must be a critical spacing or cavity density that is required for maximum heat transfer. If these cavities are too close together, the bubbles they generate interfere with each other, disturbing the fluid flow pattern over and above the test surface in such a way that the transfer of heat is reduced. Also, separating the cavities by too great a distance allows the formation of natural nucleation sites on the test surface areas between the cavities. Clearly the development of any analytical expression for this optimum cavity placement would be an extremely difficult task and one that would appear to be highly dependent upon the surface geometry and material as well as the fluid medium being utilized.

In this particular experiment it would appear that the major problem was that the cavity spacing was too large. This allowed for a considerable amount of natural nucleation on the surface and the tremendously turbulent and coalesced bubble flow above the test surface.

As can be seen from the plots of the experimental data, there was never any improvement in the heat transfer rate when the temperature was increasing and the nucleation sites were activating. This is again attributed to the natural nucleation sites that activated before the artificial cavities. Improvement was shown, however, in the situation of the temperature decreasing and the nucleation sites deactivating. In this situation it was generally observed that the artificial cavities were the last nucleation sites to deactivate.

V. CONCLUSIONS AND RECOMMENDATIONS

The results of this experiment led to the following conclusions:

(1) The surface used in this experiment performed extremely well in the investigation of saturated pool boiling heat transfer. Its value in natural convection heat transfer studies is very questionable due to the uncertainty in the natural convection heat transfer coefficient over the circumferential fin section.

(2) The artificial nucleation sites did, in fact, increase the heat transfer characteristics of the surface. Accurate determination of the critical cavity spacing must be accomplished on an ad hoc basis to ensure optimal improvements.

(3) Analytic solutions and computer models of thin circumferential fins similar to the type used in this experiment are very difficult to interpret. The strong dependence of the solution upon the convection heat transfer coefficient over the fin makes the reasonable knowledge of this coefficient a necessity.

In an effort to further understand the augmentation of heat transfer with artificial cavities, the following recommendations are made:

(1) Further tests in this area should utilize a surface similar to that used by Duncan or Penkitti [9,10] for natural convection studies and a surface similar to the one used in this experiment for boiling heat transfer studies.

(2) Experiments investigating the effects of density of constant diameter artificial nucleation sites should be conducted and an analytic expression developed that will give the cavity density required for maximum heat transfer. This should be followed by a test series investigating the effects of varying cavity diameters and cavity depths.

(3) To complete the study of the influence of artificial cavities on natural convection and boiling heat transfer, experiments should be conducted to determine the effects of these cavities when the depth of the fluid is changed from very deep pool boiling to thin film boiling. Additionally, the cavity effects should be investigated while the surface is rotated from the horizontal flat plate position to the vertical flat plate position.

(4) Thermocouples should be placed both radially and peripherally around the underside of the circumferential fin to monitor the temperature distribution in this region and to enable the experimental determination of the convection heat transfer coefficient over the fin.

APPENDIX A

THERMOCOUPLE CALIBRATION PROCEDURE

The accurate determination of the test surface and fluid temperatures was a significant part of this experiment since all the results and discussion are based on those temperatures. For this reason, precise calibration of the sheathed, bulk temperature and independent thermocouples was necessary. The entire test apparatus was calibrated as a total measurement system. Once the calibration was accomplished, none of the wiring or recording instruments of the apparatus were changed.

A Rosemount Calibration System, with a constant temperature oil bath, was used for the calibration. The reference thermocouple, sealed in a glass tube filled with oil, was placed in an electronic ice point reference junction. The six sheathed, eight bulk and one independent thermocouples were suspended several inches into the oil bath. A Platinum Resistance Thermometer in conjunction with a precision commutation bridge was used as a standard. The calibration was conducted over a range from 75°F to 300°F. A maximum error for the thermometer for this range of temperature was 0.004 millivolt.

The results of the thermocouple readings were compared with the standard thermocouple tables. The deviation from the table values ranged from +0.002 to -0.016 millivolt for

the sheathed thermocouples while the deviation from the table values ranged from +0.008 to -0.009 millivolt for the bulk temperature and independent thermocouples. The decision was made to use the reading values directly with an assigned uncertainty for the sheathed thermocouples of 0.3 ^{o}F and an uncertainty of 0.2^{o}F for the bulk temperature and independent thermocouples.

APPENDIX B

ANALYTICAL SOLUTION TO THE PROBLEM OF HEAT TRANSFER FROM A THIN CIRCUMFERENTIAL FIN WITH ONE SIDE INSULATED

The problem under consideration is that of the heat transfer from a thin circumferential fin. The analysis incorporates the use of the Bessel Function to develop a solution that will account for losses through the fin.

The geometry of the problem is as shown in figure 31. As mentioned previously, the thin fin was chosen for the expressed purpose of "choking" the heat transfer rate through the fin enabling the heat transfer rate to be greatest at the one-inch central core of the test section. Throughout the development of the solution it is assumed that the underside of the fin is perfectly insulated.

The governing equation for a circumferential fin with convection from the top only is then

$$\frac{d\theta^2}{dr^2} + \frac{1}{r}\frac{d\theta}{dr} - \frac{h}{K}\frac{1}{w}\theta = 0$$

where h = convection heat transfer coefficient

K = conduction heat transfer coefficient

$\theta = (T - T_\infty)$

The boundary conditions for the governing D.E. are

at $r = r_B$ $\quad \theta = \theta_o$

$r = \infty$ $\quad d\theta/dr = 0$

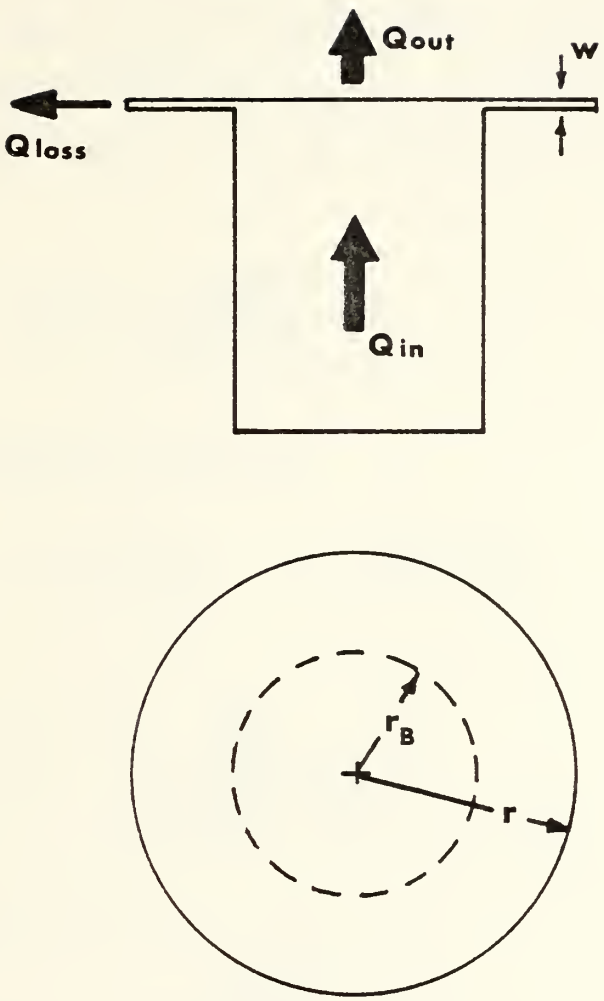

Figure 31. Problem Geometry

Solving this problem with the use of Bessel Functions yields

$$\theta = B\, I_o\left(\sqrt{\frac{h}{Kw}}\, r\right) + C\, K_o\left(\sqrt{\frac{h}{Kw}}\, r\right)$$

It is seen that as r approaches infinity, K_o approaches zero. It is also seen that as r approaches infinity, I_o becomes unbounded, which does not satisfy the boundary condition that at $r = \infty$, $d\theta/dr = 0$, and therefore B must equal zero. This leaves

$$\theta = C\, K_o\left(\sqrt{\frac{h}{Kw}}\, r\right)$$

with the boundary condition

$$r = r_B \qquad \theta = \theta_o$$

therefore

$$C = \frac{\theta_o}{K_o\left(\sqrt{\frac{h}{Kw}}\, r_B\right)}$$

Substituting for C and rearranging

$$\frac{\theta}{\theta_o} = \frac{K_o\left(\sqrt{\frac{h}{Kw}}\, r\right)}{K_o\left(\sqrt{\frac{h}{Kw}}\, r_B\right)} \qquad (1)$$

From Fourier's Law of Heat Conduction the equation governing the conduction heat transfer at the base of the fin is

$$Q = -KA \left.\frac{dT}{dr}\right|_{r=r_B}$$

or

$$Q = -KA \left.\frac{\partial\theta}{\partial r}\right|_{r=r_B}$$

From (1) it can be seen that

$$\theta = \frac{\theta_o K_o(mr)}{K_o(mr_B)}$$

where

$$m = \sqrt{\frac{h}{K_{ss} w}}$$

therefore

$$\frac{\partial \theta}{\partial r} = \theta_o \frac{1}{K_o(mr_B)} \left(-mK_1(mr)\right)$$

Substituting this into the conduction equation and evaluating at the base of the fin yields

$$\theta = -K_{ss} A \left(\frac{-\theta_o}{K_o mr_B} \left(mK_1(mr_B)\right)\right)$$

which reduces to

$$\theta = K_{ss} A \theta_o m \frac{K_1(mr_B)}{K_o(mr_B)}$$

Evaluating m

$$m = \sqrt{\frac{h}{K_{ss} w}}$$

where, for this project

w = 0.001 feet

K_{ss} = 9.03 - 9.38 BTU/hr-ft $^{\circ}$F

h = BTU/hr-ft^2 $^{\circ}$F

From graphical representation of Bessel Function behavior for the K's, it can be seen that a small argument, x=5 or less, is needed for a significant value of K. The behavior of the argument is such that as the thermal conductivity of the fin material, Kss, increases, the more difficult it is for the fin to reduce the heat transfer rate. To make a "worst case" analysis then, Kss was chosen at the high end of its range to be a value of 9.4 BTU/hr-ft ^{o}F. Inserting the appropriate values, m as a function of h becomes

$$m = 10.31\sqrt{h}$$

It was assumed that the convection heat transfer coefficient could be represented by $h \alpha \Delta Tsat^{0.3}$, a convection coefficient somewhere between laminar and turbulent natural convection.

It was also assumed that there was a five degree drop in superheat between the central section of the test surface and the base of the fin. A superheat condition, based on experimental observations as well as "worst case" objectives, of 40 degrees F was chosen.

Denoting the properties of the system directly over the test core and those over the fin with the subscripts 1 and 2 respectively, the ratio of the h's is then

$$\frac{h_2}{h_1} = \left(\frac{\Delta T_{SAT\,2}}{\Delta T_{SAT\,1}} \right)^{0.3}$$

which yields

$$\frac{h_2}{h_1} = 0.96$$

Experimental observation in this region found an h over the central portion of the test section to be on the order of 100 BTU/hr-ft F. Therefore

$$h_2 = 96 \text{ BTU/hr-ft}^2\ ^\circ\text{F}$$

Evaluating the argument of the Bessel Function yields the following:

$$x = mr_B = 4.21$$

As the temperature increases through the natural convection region into the boiling heat transfer region, the convection heat transfer coefficient increases causing the argument, x, to increase. For this reason the asymptotic behavior (large argument) of the Bessel Functions was utilized in the following form:

$$K_\nu(x) \sim \left(\frac{\pi}{2x}\right)^{\frac{1}{2}} e^{-x} \left\{ 1 + \frac{4\nu^2 - 1}{1!\ 8x} + \frac{(4\nu^2-1)(4\nu^2-3^2)}{2!\ (8x)^2} + \cdots \right\}$$

The ratio of the $K_\nu(x)$ terms is essentially a ratio of the first two terms of the series

$$\frac{K_1(mr_B)}{K_0(mr_B)} = \frac{\left(\frac{\pi}{2x}\right)^{\frac{1}{2}} e^{-x} \left(1 + \frac{3}{8x}\right)}{\left(\frac{\pi}{2x}\right)^{\frac{1}{2}} e^{-x} \left(1 - \frac{1}{8x}\right)}$$

which simplifies to

$$\frac{K_1(mr_B)}{K_0(mr_B)} = \left(\frac{8x+3}{8x-1} \right)$$

Substituting the value for the argument x

$$\frac{K_1 (m r_B)}{K_0 (m r_B)} = 1.122$$

Substituting for the ratio of the K's, the equation for the heat transfer rate at the base of the fin simplifies to

$$Q = Kss\ A\ \theta_o\ m\ (1.122)$$

where $Kss = 9.4$ BTU/hr-ft ^{o}F

$m = 101$ 1/ft

$\theta = T_o - T_\infty$ max $\Delta T \sim 40^{o}F$

$A = 2\pi r_B w = 0.00021617$ ft^2

then

$$Qloss = 11.16 \text{ BTU/hr}$$

In evaluating the heat transfer rate out of the test surface, it is assumed that there are no losses other than through the fin. An energy balance yields

$$Qin = Qout + Qloss$$

where

Qin is as measured between TC5 and TC6.

Qloss represents the losses through the circumferential fin

Qout represents the heat transfer rate to the fluid at the one-inch central core of the test surface

Using experimentally observed data for the two representative cases, i.e. natural convection and nucleate boiling heat transfer, enabled this problem solution to give an indication of performance of the fin throughout the test. For:

Case I (Natural Convection Region):

$$Qin = (4667.4)\left(\pi\frac{(\frac{1}{12})^2}{4}\right) = 25.46 \text{ BTU/hr}$$

$$Qloss = 11.16 \text{ BTU/hr}$$

$$Qout = 14.29 \text{ BTU/hr}$$

In the natural convection region, the losses represent 43.8 percent of the input to the test section.

The figure for the losses in the natural convection region is highly suspect due to the fact that the circumferential fin makes this problem a very difficult one to solve analytically. The major difficulty is what to use for the convection heat transfer coefficient in the vicinity of the fin. Additional problems arise in determining exactly what the temperature gradient is near the base of the fin. Since the convection heat transfer coefficient is a function of the temperature gradient, it is clear to see that the experimental determination of the temperature gradient in the fin is essential to the solution.

The nature of the problem is such that these two difficulties make a realistic solution a most difficult thing;

it is on the order of being a self-fulfilling problem, i.e. pick an h and ΔTsat that make the solution give the desired result.

Work with computer programs proves to be equally artificial as an approach to the solution. Since most of these programs require an arbitrary specification of h, the temperature profile and heat transfer rate are again driven to whatever results are desired.

On the basis of this analysis it is easy to see that this particular geometry is not well suited to good natural convection research. It appears that for analytical purposes and experimental observations, a surface similar to that used by Duncan or Penkitti [9,10] should be used.

Case II (Nucleate Boiling Region):

$$Q_{loss} = (9.4)(0.00021617)(45)(101)(1.22) = 12.54 \text{ BTU/hr}$$

$$Q_{in} = (17065.6)(\pi \frac{(\frac{1}{12})^2}{4}) = 93.08 \text{ BTU/hr}$$

$$Q_{out} = 80.53 \text{ BTU/hr}$$

In the boiling region the losses represent only 13.5 percent of the available heat transfer rate.

The test surface performs much better as a nucleate boiling platform. Though the same problems in specifying h and ΔTsat exist, the solution gives a good feel for the effectiveness of the fin.

APPENDIX C

UNCERTAINTY ANALYSIS

The uncertainty analysis employed in this experimental work is of the general form:

$$U_R = \left[\sum \left\{ \frac{Ex}{x} \right\}^2 \right]^{1/2}$$

where $U_R = dR/R$, the percentage uncertainty in quantity R. Ex represents the uncertainty of the xth measured quantity, and x represents the experimentally measured value for the xth quantity.

In completing the analysis, several assumptions and approximations had to be made in order to develop a reasonable estimate of the uncertainties for each variable. The following table is a summary of measured experimental quantity uncertainties:

TABLE I

Experimental Uncertainties of Variables

VARIABLE	BASIS FOR VALUE	UNCERTAINTY
Kss	Assumptions based on table values [13]	5%
Tw	Thermocouple calibration and extrapolation	0.37-0.41°F
Sheathed Thermocouples (TC1-TC6)	Thermocouple calibration	0.3°F
Unsheathed Thermocouples (TC7&TC8)	Thermocouple calibration	0.2°F
Δx	Accuracy of measurement	0.002 in
Tsat	Accuracy of Ref. [12]	0.05°F
ΔTsat	Tw and accuracy of Ref. [12]	See results page 89
q	Accuracy of Ref. [13], thermocouple calibration and physical measurements	See results page 89
h	Uncertainty in q and ΔTsat	See results page 89

The general forms of the uncertainty analysis are presented below:

For ΔTsat:

$$U_{\Delta T_{SAT}} = \frac{E_{THERMOCOUPLES}}{\Delta T_{SAT}}$$

For q:

$$U_q = \left[(U_{Kss})^2 + (U_{\Delta T})^2 - (U_{\Delta X})^2 \right]^{1/2}$$

For h:

$$U_h = \left[(U_q)^2 + (U_{\Delta T_{SAT}})^2 \right]^{1/2}$$

The following sample calculations are presented using data from test run 4. The surface contained six artificial cavities, and the best and worst case situations are represented:

BEST CASE:

$$U_{\Delta T_{SAT}} = \left[\frac{0.3}{53.6} \right] = 0.56\ \%$$

$$U_q = \left[(5)^2 + \left(\frac{0.3}{169.6} \right)^2 - \left(\frac{0.002}{0.365} \right)^2 \right]^{1/2} = 5.0\%$$

$$U_h = \left[(5)^2 + (0.56)^2 \right]^{1/2} = 5.03\ \%$$

WORST CASE:

$$U_{\Delta T_{SAT}} = \left[\frac{0.3}{1.04} \right] = 28.8\ \%$$

$$U_q = \left[(5)^2 + \left(\frac{0.3}{118.79} \right)^2 - \left(\frac{0.002}{0.365} \right)^2 \right]^{1/2} = 5.0\ \%$$

$$U_h = \left[(5)^2 + (28.8)^2 \right]^{1/2} = 29.2\%$$

TABLE II

Results of Uncertainty Analysis

All results expressed as percentage uncertainty.

SURFACE	CASE	U_{Tsat}	U_q	U_h
Blank, mirror Finished	Best	0.46	4.99	4.92
	Worst	10.0	4.99	11.18
One cavity	Best	0.44	4.99	4.92
	Worst	6.7	4.99	8.36
Seven cavity	Best	0.56	4.99	5.0
	Worst	28.8	4.99	29.2
Thirteen cavity	Best	0.48	4.99	5.02
	Worst	5.3	4.99	7.28

LIST OF REFERENCES

1. Heled, Y., Ricklis, J., and Orell, A., "Pool Boiling from Large Arrays of Artificial Nucleation Sites," Int. J. Heat Mass Transfer, v. 13, p. 503-516, March 1970.

2. Knudsen, J. G. and Katz, D. L., "Fluid Dynamics and Heat Transfer," McGraw-Hill, 1958.

3. Holman, J. P., "Heat Transfer," 3rd ed., McGraw-Hill, 1972.

4. Corty, C. and Foust, A. S., "Surface Variables in Nucleate Boiling," Chem. Eng. Progress Symposium Series, No. 17, v. 51, 1959.

5. Bergles, A. E., Chu, R. C., and Seely, J. H., "Survey of Heat Transfer Techniques Applied to Electronic Equipment," ASME 72-WA/HT-39, 1972.

6. Marto, P. J., Moulson, J. A., and Maynard, M. D., "Nucleate Pool Boiling of Nitrogen with Different Surface Conditions," Journal of Heat Transfer, p. 437-444, November 1968.

7. Shokri, M. and Judd, R. L., "Nucleation Site Activation in Saturated Boiling," Journal of Heat Transfer, p. 93-98, February 1975.

8. Chapman, R. H., "Saturated Pool and Flow Boiling Studies with Freon-113 and Water at Atmospheric Pressure," Ph.D. Thesis, University of Tennessee, ORNL-4987, November 1974.

9. Duncan, D. S., "Natural Convection Heat Transfer from a Horizontal Disk in a Cylindrical Enclosure," M.S. Thesis, Naval Postgraduate School, Monterey, California, 1971.

10. Penkitti, A., "The Influence of Artificial Cavities on Natural Convection Heat Transfer from a Horizontal Surface," M.S. Thesis, Naval Postgraduate School, Monterey, California, 1975.

11. Moulson, J. A., "Nucleate Pool Boiling of Nitrogen from Artificial Cavities," M.S. Thesis, Naval Postgraduate School, Monterey, California, 1967.

12. "Properties of Commonly-Used Refrigerants," 1957 ed., Air-Conditioning and Refrigeration Institute, 1957.

13. Touloukian, Y. S., "Thermophysical Properties of Matter," v. 1, 1970.

14. Sparrow, E. M., and Husar, R. B., "Patterns of Free Convection Flow Adjacent to Horizontal Heated Surfaces," Int. Journal Heat Mass Transfer, v. 11, No. 7, p. 1206-1208, July 1968.

15. Nail, J. P., Vachon, R. I., and Morehouse, J., "An SEM Study of Nucleation Sites in Pool Boiling from 304 Stainless Steel," Journal of Heat Transfer, p. 132-137, May 1974.

INITIAL DISTRIBUTION LIST

		No. Copies
1.	Library, Code 0142 Naval Postgraduate School Monterey, California 93940	2
2.	Department Chairman, Code 69 Department of Mechanical Engineering Naval Postgraduate School Monterey, California 93940	1
3.	Assoc. Professor M. D. Kelleher Department of Mechanical Engineering Naval Postgraduate School Monterey, California 93940	6
4.	Lieutenant George R. Yount, USN c/o Supervisor of Shipbuilding Conversion and Repair, USN Newport News, Virginia 23607	3
5.	Defense Documentation Center Cameron Station Alexandria, Virginia 22314	2

Thesis
Y78
c.1
168500
Yount
The influence of drilled cavities on natural convection and saturated pool boiling heat transfer from a horizontal surface.